RELATION BETWEEN FLAME SPEED AND STRETCH FOR A PREMIXED FLAME IN A STAGNATION POINT FLOW

BY

MIDHUN JACOB JOY

THESIS

Submitted in partial fulfillment of the requirements
for the degree of Master of Science in Mechanical Engineering
in the Graduate College of the
University of Illinois at Urbana-Champaign, 2017

Urbana, Illinois

Advisor:

Professor Moshe Matalon

ABSTRACT

Displacement speed of a flame is a hydrodynamic concept, and it is defined as the normal component of the velocity of the incoming flow evaluated on the unburned side of the flame. Except for a steadily propagating flame with zero stretch (planar flame), this definition is ambiguous because the mass flux and, consequently, the gas velocity vary across the thickness of the flame represented by the flame/thermo-diffusive/pre-heat zone. In other words, the flame displacement speed has different values when evaluated at different locations within the flame zone. This has led to confusion about the position within the flame that must be used for measuring flame speed. Additionally, according to the hydrodynamic theory, the flame speed of weakly stretched flames is dependent on the flame stretch and the position/isotherm chosen within the flame zone through a parameter known as the Markstein Length. It is the objective of this study to provide a recommendation for the position/isotherm within the flame zone for measuring gas velocity in experiments that provides a flame speed value consistent with the hydrodynamic theory. In this regard, a premixed flame in an axisymmetric laminar stagnation point flow is studied using the hydrodynamic theory. First, the outer or hydrodynamic solution is obtained by solving modified Euler equations along with jump conditions resulting from conservation laws. Thereafter, the structure of the flame zone is resolved by rescaling the coordinate and the inner solution obtained using asymptotic theory is presented. Having obtained the outer and inner solutions, a uniformly valid composite expression for the mass flux across the flame is derived and presented. Finally, flame speeds are evaluated at different isotherms/positions within the flame zone, and a recommendation for the position to measure gas velocity in experiments is provided.

Dedicated to my family ...

ACKNOWLEDGEMENTS

This work would not have been possible without the help and guidance of my advisor, Professor Moshe Matalon, who helped me understand the importance of systematic approach to solving asymptotic problems and kept me motivated throughout my time as a graduate student at the University of Illinois. I am also grateful to my fellow graduate students Shikhar Mohan and Advitya Patyal for helping me a great deal with the formatting of my thesis. I would also like to thank the Department of Mechanical Science and Engineering for providing me funding for the entire duration of my study through teaching assistantships. Further, I would like to thank my parents for believing in me and especially for financially supporting my education all the way from kindergarten to undergraduate college. Last but not the least, I would like to thank God for all the blessings I have received in my life.

TABLE OF CONTENTS

LIST OF FIGURES

Chapter 1

INTRODUCTION

A flame in a flow field has an ordered multi-layer structure where the different layers have different dominant processes. The different layers or zones and the corresponding dominant processes are (i) the outer or hydrodynamic zone where advection is the dominant process, (ii) the flame or thermo-diffusive zone where diffusion (thermal and molecular) is the dominant process, and (iii) the reaction zone where chemical kinetics is the dominant process. Figure 1.1 below shows the structure of a flame in a flow field. The length scales associated with the hydrodynamic, thermo-diffusion and reaction layers are L, $l_f = \mathcal{D}_{th}/S_L$, and $l_r = l_f/\beta$ respectively, where $\mathcal{D}_{th} = \frac{\lambda}{\rho_u c_p}$, is the thermal diffusivity, S_L is the laminar flame speed and $\beta = \frac{E_a(\tilde{T}_a - \tilde{T}_u)}{R\tilde{T}_a{}^2}$ is the Zel'dovich number (typically, $\beta \approx 10$). The reaction layer is an order of magnitude smaller in size than the thermo-diffusive layer, which in turn is an order of magnitude smaller in size compared to the characteristic length of the hydrodynamic flow field. When viewed from a length scale relevant to the flow field, i.e. in the limit $\delta = \frac{l_f}{L} \to 0$, the thermo-diffusive layer and reaction layer reduce to an interface called flame front that separates the unburned and burned gases [1].

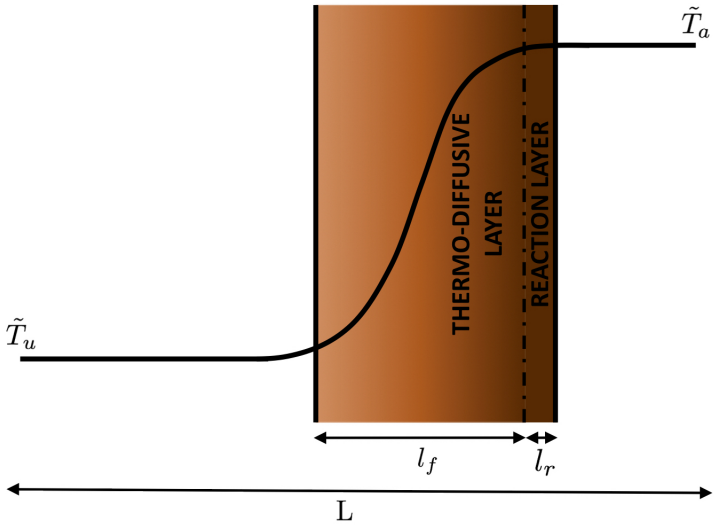

Figure 1.1: Structure of a Flame

Hydrodynamic theory of flame propagation treats a flame as an interface separating the un-

burned and burned gases [2]. The mass flux and other gas properties like temperature and density suffer jumps across this interface in order to satisfy the conservation laws. According to the theory, the flame displacement speed or FDS is defined as the propagation speed of the flame relative to the unburned gas. It is evaluated as the difference between the normal component of the velocity of the unburned gas evaluated at the flame front location and velocity of the flame in a fixed coordinate system [1]. Mathematically,

$$S_f = \mathbf{u}.\hat{\mathbf{n}}|_{n=0^-} - V_f \tag{1.1}$$

where $\mathbf{u}$ is the velocity, $\hat{\mathbf{n}}$ is the unit normal pointing towards the burned gas and V_f is propagation speed of the flame in a fixed frame of reference.

This expression for flame speed is unique only in a hydrodynamic context or for steadily propagating planar flames, and it corresponds to the laminar flame speed (S_L) - a property of the reactant mixture. By definition, a planar flame is unstretched. Flame stretch is a measure of the flame front deformation resulting from its propagation and stresses in the flow surrounding it [1] [3]. It is evaluated as:

$$\mathbb{K} = \frac{1}{A}\frac{dA}{dt} \tag{1.2}$$

where A is an infinitesimal area formed by points that remain on the flame surface. Alternatively, within the context of hydrodynamic theory (when $S_f \approx S_L$), the stretch rate can be expressed as [3]:

$$\mathbb{K} = \kappa S_L + \mathbb{K}_s \tag{1.3}$$

where $\kappa = -\nabla.\hat{\mathbf{n}}$ is the flame front curvature, $\mathbb{K}_s = -\hat{\mathbf{n}}.\mathbf{E}.\hat{\mathbf{n}}$ is the hydrodynamic strain in flow field and S_L is the laminar flame speed - a property of the reactant mixture.

Figure 1.2 shows the essential difference between unstretched and stretched flames. Steadily propagating planar flames are unstretched and have the same mass flux across the entire flame zone. On the other hand, stretched flames have normal mass fluxes that change across the flame zone due to lateral fluxes and accumulation within the flame [4]. In the figure below, there are two normals (n_1 and n_2) and two isotherms (T_1 and T_2) at two transverse/tangential positions '1' and '2' respectively within the flames. In the planar case, there is no lateral flux or accumulation of

mass, and the flame speeds evaluated at isotherms T_1 and T_2 will be the same. However, in the stretched case, there may be lateral fluxes and accumulation of mass (as indicated by the direction of the normals). In other words, the mass flux evaluated at isotherm T_1 at transverse position '1' has a component that will contribute to the normal component of the mass flux at isotherm T_2 at transverse position '2.' Therefore, the flame speed evaluated at isotherm T_1 will be different from that evaluated at isotherm T_2.

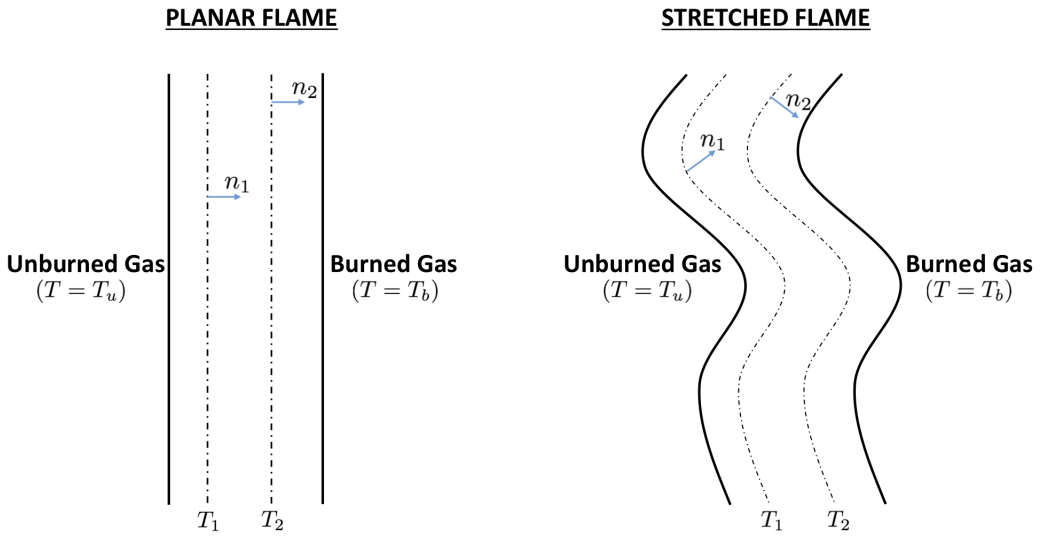

Figure 1.2: Planar and Stretched Flames

Markstein proposed a modified expression for flame speed of weakly stretched flames where a parameter called Markstein Length ($\mathcal{L}$) factors the effect of stretch on flame speed [2].

$$S_f = S_L - \mathcal{L}\mathbb{K} \tag{1.4}$$

Although the flame speed is conventionally defined with respect to the unburned gas, it can also be defined with respect to the burned gas. Consequently, two Markstein Lengths $\mathcal{L}^u$ and $\mathcal{L}^b$ can be evaluated on the unburned and burned sides respectively. Depending on the region (unburned or burned) with respect to which the flame displacement speed is measured, the unburned or burned side Markstein length must be used in equation (1.4) [1]. As can be seen from the equation (1.4) above, the flame speed of weakly stretched flames varies linearly with flame stretch; in particular,

it depends on (a) the extend of flame stretch and (b) the sign for $\mathcal{L}$. Markstein Length ($\mathcal{L}$) is a parameter that is of the order of magnitude of the thickness of a flame and has been shown to depend on Lewis number and thermal expansion parameter (σ) [5]. Typically, $\mathcal{L}$ is negative for Lewis number less than approximately unity, and $\mathcal{L}$ is positive for Lewis numbers greater than approximately unity [6]. Another result that follows from the above equation is that the flame speed at zero stretch should be equal to the laminar flame speed. Even though the Markstein length is an order δ quantity and the thickness of the flame is small, the change in Markstein length across the flame zone may be an O(1) quantity [7]. This would lead to significantly different flame speeds when equation (1.4) is used to evaluate the flame displacement speed (FDS) at different positions within the flame zone.

Physically, a flame has a finite thickness. Consequently, experimentalists are faced with the difficulty of choosing a location/isotherm within the flame for measuring the flame speed. In addition, experimentalists measure the flame speed of stretched flames and extrapolate that to zero stretch to estimate the laminar flame speed. A number of experimental studies showed that depending on the isotherm or reference location chosen to measure the gas velocity, the flame speed recovered by extrapolation to zero stretch was different [1]. These contradicting experimental results led to confusion about the validity of equation (1.4) and the reference location that must be chosen.

This study focuses on presenting a uniformly valid composite expression for the gas velocity across a stagnation point flame and providing a recommendation for the location to be chosen for evaluation of flame speed. The hydrodynamic solution to the flow field on either side of the premixed stagnation point flow flame is presented first. Thereafter, the flame zone or inner solution is applied to the problem, and the hydrodynamic and inner solutions are matched to obtain composite expressions for the mass flux and gas velocity valid everywhere except the reaction zone. Finally, the density weighted flame speed is evaluated at different locations within the flame using the composite expression for mass flux, and a recommendation is provided for the reference location within the flame zone where measurement of gas velocity would lead to results consistent with equation (1.4).

Chapter 2

OUTER FLOW

2.1 SPECIFICATION

The flow being studied is that around a bluff body like a cylinder in the vicinity of the cylinder's upstream stagnation point. The incoming flow is axisymmetric and has a prescribed strain rate (ϵ). It is assumed that a premixed flame is stabilized in the flow field at some location (d), that is yet to be determined, before the stagnation point. Physically, such a flow field can be achieved by using a circular burner that is kept some distance away from a flat plate. Alternatively, a counter-flow setup where the flow of interest impinges against an opposing flow of some inert gas could be used. After an initial transient, when the strain rate is sufficiently high, the flame detaches from the surface of the burner and stabilizes in the flow field at a distance (d) away from the plate. The figure below shows a schematic of the flow configuration.

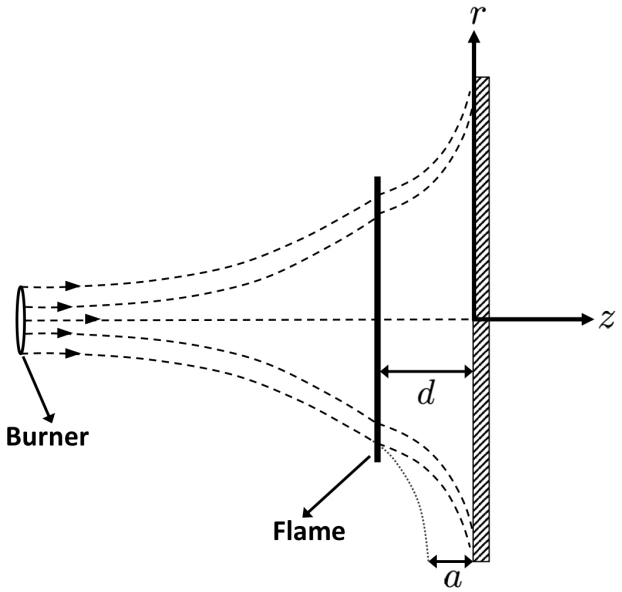

Figure 2.1: Schematic Showing Flow Setup

The velocity field for the flow is described as $\mathbf{u} = u\hat{e}_z + v\hat{e}_r$ where u is the axial velocity and

v is the radial velocity, and $\hat{e}_z$ and $\hat{e}_r$ are unit vectors in the axial and radial directions. These velocities are prescribed as:

$$u = -2\epsilon(z + a) \tag{2.1}$$

$$v = \epsilon r \tag{2.2}$$

where ϵ is the strain rate. This flow conforms with the general form proposed by Howarth [8].

Because of the presence of the flame, the incoming flow is offset by a distance (a) so as to ensure that the velocity indeed goes to zero at the wall of the bluff body. For this axisymmetric flow configuration, the unit normal, $\hat{\mathbf{n}} = \hat{e}_z$, and since the flame is not moving, $V_f = 0$. Therefore, from equation (1), the flame displacement speed reduces to

$$S_f = u\Big|_{d^-} = -2\epsilon(z + a)\Big|_{z=-d^-} \tag{2.3}$$

Since the flow is axisymmetric, the flame is flat, and the curvature term, $\kappa = -\nabla.\hat{\mathbf{n}}$, is identically zero. This means that only the strain rate in the flow field contributes to flame stretch in the case of a stagnation point flame. The hydrodynamic strain rate is evaluated as $\mathbb{K}_s = -\hat{e}_z.\mathbf{E}.\hat{e}_z$ where the strain tensor, $\mathbf{E} = \frac{1}{2}[(\nabla\mathbf{u}) + (\nabla\mathbf{u})^T]$. This reduces to $\mathbb{K}_s = -\dfrac{du}{dz} = 2\epsilon$, and therefore,

$$\mathbb{K} = 2\epsilon \tag{2.4}$$

As mentioned before, the hydrodynamic theory treats the flame as an interface across which the mass flux, velocity, temperature and density suffer jumps. As a consequence of treating the flame as an interface, the flow on each side of the flame can be solved separately and then be related using jump conditions derived for finite thickness interfaces. In addition, the reaction terms can be ignored because all of the reaction is confined to the flame sheet, and the density and temperature can be treated as piecewise constant. Further, the viscosity(μ) and thermal conductivity (λ) are evaluated as mixture averages and are assumed to be constant on either side of the flame sheet. The governing equations on each side can be derived from the steady-state continuity and Navier-Stokes equations:

$$\text{Mass:} \quad \tilde{\nabla}.\tilde{\mathbf{u}} = 0$$

$$\text{Momentum:} \quad \tilde{\rho}(\tilde{\mathbf{u}}.\tilde{\nabla})\tilde{\mathbf{u}} = -\tilde{\nabla}\tilde{p} + \tilde{\mu}[\tilde{\nabla}^2\tilde{\mathbf{u}}] + \tilde{\rho}\mathbf{g}$$

The densities and temperatures on the unburned and burned sides are related by the thermal expansion parameter (σ).

$$\sigma = \frac{\rho_u}{\rho_b} = \frac{T_b}{T_u} \tag{2.5}$$

where ρ_u and ρ_b are the densities of the unburned and burned gas respectively, and T_u and T_b are the temperatures of the unburned and burned gas respectively. To non-dimensionalize, S_L, ρ_u, T_u are used as the scales for velocity, density and temperature respectively, and $L = \frac{S_L D}{U}$ is used as the scale for length. Further, $\tilde{\epsilon}$ is non-dimensionalized using the parameter U/D which represents a strain rate. The resulting non-dimensionalized equations are:

$$\nabla.\mathbf{u} = 0 \tag{2.6}$$

$$\rho(\mathbf{u}.\nabla)\mathbf{u} = -\nabla p + \delta Pr\nabla^2\mathbf{u} \tag{2.7}$$

Non-dimensionalizing equation (1.4) gives

$$S_f = 1 - \delta\alpha\mathbb{K} \tag{2.8}$$

where, $\delta\alpha$ is the Markstein Length $\mathcal{L}$ in non-dimensional form[1][7]. It should be noted that equations (2.1), (2.2) and (2.4) take the same form in the non-dimensional case. Further, the Froude number is assumed to be large, and therefore, the gravitational force term which is multiplied by the square of the inverse of Froude number is dropped. Although the incoming flow is prescribed to be irrotational, vorticity is generated at the flame, and the flow of the burned gas is rotational. In order to solve for the flow field on the burned side, all the variables are expanded asymptotically using the non-dimensional flame thickness, δ, as the small parameter. That is,

$$u = u_0 + \delta u_1 + O(\delta^2), \qquad v = v_0 + \delta v_1 + O(\delta^2), \qquad a = a_0 + \delta a_1 + O(\delta^2)$$
$$d = d_0 + \delta d_1 + O(\delta^2), \qquad T = T_0 + \delta T_1 + O(\delta^2), \qquad \omega = \omega_0 + \delta\omega_1 + O(\delta^2)$$

and so on for all other variables.

Typical values of flame thickness for deflagrations are around 0.001m, and typical values for

[1] α, defined in the section 3.1, is the parameter that accounts for reactant properties through an effective Lewis number (Le_{eff}).

the laminar flame speed (S_L) are of the order of 0.1m/s. This implies that the non-dimensional flame thickness (δ) is of the order of 10^{-2}. This study considers a flame that is stabilized at a location well outside the viscous boundary layer next to the wall. Therefore, the non-dimensional flame thickness (δ) should be an order of magnitude lower than the non-dimensional flame stand-off distance (d). Unless otherwise stated, a value of $\delta = 0.025$ and $\epsilon = 2$ is used for all the calculations and plots presented hereafter.

In order to solve for the outer flow solution on the burned side of the flame sheet, jump conditions across the flame sheet need to be derived for the quantities of interest. The section below provides an outline of the method used to derive these jump conditions, both across the flame standoff location (d) and leading order flame location (d_0).

2.2 JUMP CONDITIONS

Jump in a quantity across a flame signifies the difference between its values on the burned and unburned sides of the flame sheet respectively. This section presents the jumps in the flow variables across the flame at its stand-off distance (d) and, for convenience, at the leading order stand-off distance (d_0).

2.2.1 Across the Flame (d):

The jump conditions that result from applying the conservation of momentum equations to an interface separating fluids with negligible viscosity are known as *Rankine-Hugoniot* jump relations. If viscous effects are included as $O(\delta)$ terms and the interface is assumed to be stationary (which is the case for this study), then the resulting jump relations across the flame have correction terms of $O(\delta)$ and are given as [9]:

$$\begin{aligned}
[\![\rho(\mathbf{u}.\hat{\mathbf{n}})]\!] &= \delta\left(\frac{\sigma-1}{\sigma}\right)\gamma_1\mathbb{K} \\
[\![\hat{\mathbf{n}}\times(\mathbf{u}\times\hat{\mathbf{n}})]\!] &= \delta\left\{-(\lambda_b Pr+\gamma_1)\,[\![\hat{\mathbf{n}}\times\nabla\times\mathbf{u}]\!]+Pr(\lambda_b-1)\left|\frac{\partial u}{\partial r}+\frac{\partial v}{\partial z}\right|_{z=-d}\right\} \\
[\![p+\rho(\mathbf{u}.\hat{\mathbf{n}})^2]\!] &= \delta\left\{\gamma_1\,[\![\nabla p.\hat{\mathbf{n}}]\!]+2Pr(\lambda_b-1)\mathbb{K}_s\right\}
\end{aligned}$$

It can be seen from the above equations that the jump relations depend on the transport

coefficients (represented by λ) and their variation with temperature. When the thermal properties are constant, $\lambda = \lambda_b = 1$. The general relations presented above can further be simplified for an axisymmetric stagnation flow, and the resulting jump relations are[2]:

$$\text{Mass flux:} \quad [\![\rho u]\!] = 2\epsilon\delta\left(\frac{\sigma-1}{\sigma}\right)\gamma_1 \tag{2.9}$$

$$\text{Tangential velocity:} \quad [\![v]\!] = \delta(\lambda_b Pr + \gamma_1)[\![\omega]\!] \tag{2.10}$$

$$\text{Pressure:} \quad \left[\!\left[p + \rho u^2\right]\!\right] = \delta\left\{\gamma_1\left[\!\left[\frac{\partial p}{\partial z}\right]\!\right] + 4\epsilon Pr(\lambda_b - 1)\right\} \tag{2.11}$$

Since the hydrodynamic model treats density as a piecewise constant quantity, the jump in density can be evaluated as the difference between the burned and unburned densities. In non-dimensional form,

$$[\![\rho]\!] = \frac{1}{\sigma} - 1 \tag{2.12}$$

The jump in a product of quantities across an interface (flame) can be evaluated as the product of one quantity evaluated on the burned side and the jump in the other quantity added to the product of the other quantity evaluated on the unburned side and the jump in the first quantity. That is,

$$[\![AB]\!]_n = A\Big|_{n^+} B\Big|_{n^+} - A\Big|_{n^-} B\Big|_{n^-}$$

Adding and subtracting $A\Big|_{n^+} B\Big|_{n^-}$ to the above equation

$$\implies \qquad [\![AB]\!]_n = A\Big|_{n^+} [\![B]\!]_n + B\Big|_{n^-} [\![A]\!]_n$$

Using this relation and equation (2.12) in equation (2.9) gives

$$[\![\rho u]\!] = \rho\Big|_{d^+} [\![u]\!] + u\Big|_{d^-} [\![\rho]\!]$$

$$\implies \qquad 2\epsilon\delta\left(\frac{\sigma-1}{\sigma}\right)\gamma_1 = \frac{1}{\sigma}[\![u]\!] - \left(\frac{1}{\sigma}-1\right)2\epsilon(z+a)\Big|_{z=-d}$$

Substituting for the non-dimensional flame speed relation (2.8) gives

$$2\epsilon\delta\left(\frac{\sigma-1}{\sigma}\right)\gamma_1 = \frac{1}{\sigma}[\![u]\!] + \left(\frac{1}{\sigma}-1\right)(1 - \delta\alpha\mathbb{K})$$

[2] γ_1 is a definite integral defined in section 3.1

Therefore,

$$[\![u]\!] = \sigma - 1 + 2\epsilon\delta(\sigma-1)(\gamma_1-\alpha) + O(\delta^2) \tag{2.13}$$

From equation (2.11), it can be seen that the jump in pressure across the flame depends on the jump in ρu^2, which can be evaluated as either $[\![\rho(u^2)]\!]$ or $[\![(\rho u)u]\!]$. Evaluating $[\![u^2]\!]$ as $[\![u]\!]^2 + 2u\Big|_{d^-}[\![u]\!]$, we get

$$[\![u^2]\!] = \sigma^2 - 1 + 4\epsilon\delta[(\sigma^2-\sigma)\gamma_1 - (\sigma^2-1)\alpha] + O(\delta^2)$$

Using equation (2.11) after evaluating $[\![\rho u^2]\!]$ using the expansion shown above, we get for pressure:

$$[\![p]\!] = 1 - \sigma + \delta\left\{\gamma_1\left[\!\left[\frac{\partial p}{\partial z}\right]\!\right] + 4\epsilon\left[(\sigma-1)(\alpha-\gamma_1) + Pr(\lambda_b-1)\right]\right\} + O(\delta^2) \tag{2.14}$$

Vorticity is defined as $\mathbf{w} = \nabla \times \mathbf{u} = \omega\hat{e}_\theta$. Since the flow is axisymmetric, it follows that

$$\omega = \frac{\partial v}{\partial z} - \frac{\partial u}{\partial r}$$

Thus, the jump in vorticity across the flame, $[\![\omega]\!] = \left[\!\left[\frac{\partial v}{\partial z}\right]\!\right] - \left[\!\left[\frac{\partial u}{\partial r}\right]\!\right]$, where the second term can be expressed as $\frac{\partial}{\partial r}[\![u]\!]$, and since it is known from equation (2.13) that $[\![u]\!]$ is not a function of r, this term is identically 0. Therefore, $[\![\omega]\!] = \left[\!\left[\frac{\partial v}{\partial z}\right]\!\right]$.

In order to find the jump in the axial gradient of the radial velocity, the jump in all terms of the radial momentum equation is evaluated. The radial momentum equation can be obtained from equation (2.7) as

$$\rho u\frac{\partial v}{\partial z} + \rho v\frac{\partial v}{\partial r} = -\frac{\partial p}{\partial r} + \delta Pr\left[\frac{\partial^2 v}{\partial z^2} - \frac{v}{r^2} + \frac{1}{r}\frac{\partial}{\partial r}\left(r\frac{\partial v}{\partial r}\right)\right]$$

Evaluating the jumps across the flame for each term in the radial-momentum equation gives:

$$\begin{aligned}
\left[\!\left[\rho u\frac{\partial v}{\partial z}\right]\!\right] &= \left[1 + 2\epsilon\delta\left\{\left(\frac{\sigma-1}{\sigma}\right)\gamma_1 - \alpha\right\}\right]\left[\!\left[\frac{\partial v}{\partial z}\right]\!\right] \\
\left[\!\left[\rho v\frac{\partial v}{\partial r}\right]\!\right] &= \epsilon^2 r\left(\frac{1-\sigma}{\sigma}\right) + \delta\left\{\frac{\epsilon(\lambda_b Pr + \gamma_1)}{\sigma}\left[\!\left[\frac{\partial v}{\partial z}\right]\!\right] + \frac{\epsilon r(\lambda_b Pr + \gamma_1)}{\sigma}\frac{\partial}{\partial r}\left[\!\left[\frac{\partial v}{\partial z}\right]\!\right]\right\} \\
\left[\!\left[\frac{\partial p}{\partial r}\right]\!\right] &= \frac{\partial}{\partial r}[\![p]\!] = 0 + O(\delta^2) \\
\left[\!\left[Pr\frac{\partial^2 v}{\partial z^2} - Pr\frac{v}{r^2}\right]\!\right] &= Pr\left[\!\left[\frac{\partial^2 v}{\partial z^2} - \frac{v}{r^2}\right]\!\right] = O(\delta) \\
\left[\!\left[\frac{Pr}{r}\frac{\partial}{\partial r}\left(r\frac{\partial v}{\partial r}\right)\right]\!\right] &= 0 + O(\delta)
\end{aligned}$$

It should be noted that the terms multiplied by the Prandtl number (Pr) are already $O(\delta)$, and thus, the jumps in these terms would be $O(\delta^2)$ or smaller. Solving for $\left[\!\left[\frac{\partial v}{\partial z}\right]\!\right]$ from the above jump relations gives for vorticity,

$$[\![\omega]\!] = \epsilon^2\left(\frac{\sigma-1}{\sigma}\right)r - 2\epsilon^3\delta\left\{\left(\frac{\sigma-1}{\sigma}\right)\left[\left(\frac{\sigma-1}{\sigma}\right)\gamma_1 - \alpha\right]r + \left(\frac{\sigma-1}{\sigma^2}\right)(\lambda_b Pr + \gamma_1)r\right\} + O(\delta^2) \tag{2.15}$$

2.2.2 Across d_0:

The location of the flame is asymptotically approximated by $d_0 + \delta d_1$. It is convenient to express the jump relations derived in equations (2.9) through (2.15) above as jumps over the leading order flame stand-off position $z = -d_0$ as opposed to evaluating them at $z = -d$. This is done using a Taylor Series expansion as shown below:

$$[\![A_0 + \delta A_1]\!]_{n_0+\delta n_1} = [\![A_0]\!]_{n_0} + \delta\left\{[\![A_1]\!]_{n_0} + n_1\left[\!\left[\frac{\partial A_0}{\partial n}\right]\!\right]\right\}$$

Evaluating the jumps in u, v, p and ω using the above expression and comparing with jumps in these quantities across the flame (d) derived above (equations (2.13), (2.10), (2.14) and (2.15) respectively) yields the following jump conditions across d_0.

Axial Velocity:

$$[\![u_0]\!] = \sigma - 1 \tag{2.16}$$

$$[\![u_1]\!] = 2\epsilon[\sigma-1][\gamma_1-\alpha] + d_1\left[\!\left[\frac{\partial u_0}{\partial z}\right]\!\right] \tag{2.17}$$

Transverse Velocity:

$$[\![v_0]\!] = 0 \tag{2.18}$$

$$[\![v_1]\!] = (\lambda_b Pr + \gamma_1)\,[\![\omega_0]\!] + d_1\left[\!\left[\frac{\partial v_0}{\partial z}\right]\!\right] \tag{2.19}$$

Pressure:

$$[\![p_0]\!] = 1 - \sigma \tag{2.20}$$

$$[\![p_1]\!] = 4\epsilon\left[(\sigma-1)(\alpha-\gamma_1) + Pr(\lambda_b-1)\right] + (\gamma_1+d_1)\left[\!\left[\frac{\partial p_0}{\partial z}\right]\!\right] \tag{2.21}$$

Vorticity:

$$[\![\omega_0]\!] = \epsilon^2\left(\frac{\sigma-1}{\sigma}\right)r \tag{2.22}$$

$$[\![\omega_1]\!] = -2\epsilon^3\left(\frac{\sigma-1}{\sigma^2}\right)\Big[\sigma(\gamma_1-\alpha) + \lambda_b Pr\Big]r + d_1\Big[\!\Big[\frac{\partial\omega_0}{\partial z}\Big]\!\Big] \tag{2.23}$$

2.3 OUTER SOLUTION

As mentioned earlier, the flow on the unburned side of the flame in this study is irrotational. Therefore, the vorticity is zero on the unburned side, and the jump conditions (2.22) and (2.23) give the expressions for the vorticity on burned side at $z=-d_0$. As a first step towards obtaining the flow field on the burned side, the vorticity equation is obtained by taking the curl of the momentum equation (2.7).

$$\mathbf{u}(\nabla.\mathbf{w}) + (\mathbf{w}.\nabla)\mathbf{u} - (\mathbf{u}.\nabla)\mathbf{w} = \frac{1}{\rho}\delta Pr\nabla^2\mathbf{w} \tag{2.24}$$

Since the flow on the unburned side is potential and vorticity exists only in the azimuthal direction, equation (2.24) can be simplified by considering the azimuthal component with $\rho = \rho_b$. This gives

$$u\frac{\partial\omega}{\partial z} + v\frac{\partial\omega}{\partial r} - \frac{\omega v}{r} = \delta\sigma Pr\nabla^2\omega$$

Dividing by r and simplifying after plugging in asymptotic expansions accurate to O(δ) for the variables

$$\implies \quad (u_0+\delta u_1)\frac{\partial}{\partial z}\Big(\frac{\omega_0+\delta\omega_1}{r}\Big) + (v_0+\delta v_1)\frac{\partial}{\partial r}\Big(\frac{\omega_0+\delta\omega_1}{r}\Big) = \delta\sigma Pr\left[\frac{\partial^2\omega_0}{\partial z^2} + \frac{\partial}{\partial r}\Big(\frac{1}{r}\frac{\partial}{\partial r}(r\omega_0)\Big)\right]$$

Separating the terms according to order of magnitude yields:

$$\text{O(1):} \qquad u_0\frac{\partial}{\partial z}\Big(\frac{\omega_0}{r}\Big) + v_0\frac{\partial}{\partial r}\Big(\frac{\omega_0}{r}\Big) = 0 \tag{2.25}$$

$$\text{O}(\delta)\text{:}\ u_0\frac{\partial}{\partial z}\Big(\frac{\omega_1}{r}\Big) + v_0\frac{\partial}{\partial r}\Big(\frac{\omega_1}{r}\Big) + u_1\frac{\partial}{\partial z}\Big(\frac{\omega_0}{r}\Big) + v_1\frac{\partial}{\partial r}\Big(\frac{\omega_0}{r}\Big) = \sigma Pr\left[\frac{\partial^2\omega_0}{\partial z^2} + \frac{\partial}{\partial r}\Big(\frac{1}{r}\frac{\partial}{\partial r}(r\omega_0)\Big)\right] \tag{2.26}$$

As suggested Eteng et al, expressing the variables u, v and ω in terms of a streamfunction Ψ makes the mathematical derivations much more convenient [10]. The streamfunction is also asymptotically expanded as $\Psi = \Psi_0 + \delta\Psi_1 + O(\delta^2)$, and the flow variables are expressed as:

$$u = -\frac{1}{r}\frac{\partial\Psi}{\partial r} \tag{2.27}$$

$$v = \frac{1}{r}\frac{\partial\Psi}{\partial z} \tag{2.28}$$

$$\omega = \frac{1}{r}\frac{\partial^2 \Psi}{\partial z^2} + \frac{\partial}{\partial r}\left(\frac{1}{r}\frac{\partial \Psi}{\partial r}\right) \tag{2.29}$$

From equation (2.25), it can be seen that $\frac{\omega_0}{r}$ is a constant along streamlines on the burned side of the flame. However, from the jump relation (2.22), it is known that $\frac{\omega_0}{r} = \epsilon^2\left(\frac{\sigma-1}{\sigma}\right)$ at the flame ($z{=}{-}d_0$), and therefore $\frac{\omega_0}{r}$ is constant everywhere on the burned side. This suggests seeking a solution of the form $\Psi_0 = r^2 F_0(z)$. Substituting this in equation (2.25) gives $F_0'''(z) = 0$ which is confirmed by the fact that $F_0''(z) = \epsilon^2\left(\frac{\sigma-1}{\sigma}\right)$ obtained from equation (2.29). Integrating twice with respect to the axial coordinate z gives:

$$F_0(z) = \frac{\epsilon^2}{2}\left(\frac{\sigma-1}{\sigma}\right)z^2 + c_1 z + c_2$$

which can be solved subject to the following boundary conditions:

$$u_0 \; at \; (z{=}{-}d_0) = \sigma \implies F_0(-d_0) = -\frac{\sigma}{2}$$
$$v_0 \; at \; (z{=}{-}d_0) = \epsilon r \implies F_0'(-d_0) = \epsilon$$
$$u_0 \; at \; (z{=}0) = 0 \implies F_0(0) = 0$$

Solving this boundary value problem gives

$$d_0 = \frac{\sigma}{\epsilon(\sqrt{\sigma}+1)} \tag{2.30}$$

$$F_0(z) = \frac{\epsilon^2}{2}\left(\frac{\sigma-1}{\sigma}\right)z^2 + \epsilon\sqrt{\sigma}z \tag{2.31}$$

Having obtained F_0, and thereby Ψ_0, all other flow variables can be calculated to the leading order. Plugging in the value of ω_0 simplifies equation (2.26) as

$$u_0\frac{\partial}{\partial z}\left(\frac{\omega_1}{r}\right) + v_0\frac{\partial}{\partial r}\left(\frac{\omega_1}{r}\right) = 0$$

which means that $\frac{\omega_1}{r}$ is also constant along the streamlines on the burned side. In addition, evaluation of the jump relation (2.23) gives the expression, $\frac{\omega_1}{r} = -2\epsilon^3\left(\frac{\sigma-1}{\sigma^2}\right)[\sigma(\gamma_1-\alpha) + \lambda_b Pr]$, at the leading order position of the flame ($z{=}{-}d_0$). Since $\frac{\omega_1}{r}$ is also constant everywhere on the burned side of the flame, a similar approach is used, and a solution of the form $\Psi_1 = r^2 F_1(z)$ is seeked. This results in the expression $F_1'' = -2\epsilon^3\left(\frac{\sigma-1}{\sigma^2}\right)[\sigma(\gamma_1-\alpha) + \lambda_b Pr]$, which when integrated twice with respect to z gives:

$$F_1(z) = -\epsilon^3\left(\frac{\sigma-1}{\sigma^2}\right)[\sigma(\gamma_1-\alpha) + \lambda_b Pr]z^2 + c_1 z + c_2$$

This equation can be solved subject to the following boundary conditions:

$$u_1 \; at \; (z{=}{-}d_0) = 2\epsilon[\sigma{-}1][\gamma_1{-}\alpha] + d_1\left[2\epsilon^2\left(\frac{\sigma{-}1}{\sigma}\right)d_0 - 2\epsilon\sqrt{\sigma} - 2\epsilon\right] - 2\epsilon\,[d_1{+}\alpha]$$

$$\implies F_1(-d_0) = -\epsilon\,[(\sigma-1)\gamma_1 - \sigma\alpha - d_1]$$

$$v_1 \; at \; (z{=}{-}d_0) = (\lambda_b Pr + \gamma_1 + d_1)\epsilon^2\left(\frac{\sigma{-}1}{\sigma}\right)r$$

$$\implies F_1'(-d_0) = \epsilon^2\left(\frac{\sigma{-}1}{\sigma}\right)(\lambda_b Pr + \gamma_1 + d_1)$$

$$u_1 \; at \; (z{=}0) = 0 \implies F_1(0) = 0$$

Solving gives

$$d_1 = \frac{2\sigma{-}\sqrt{\sigma}{-}1}{\sqrt{\sigma}{+}1}\gamma_1 - \frac{\sqrt{\sigma}{-}1}{\sqrt{\sigma}{+}1}\lambda_b Pr - \frac{2\sigma}{\sqrt{\sigma}{+}1}\alpha \tag{2.32}$$

$$F_1(z) = -\epsilon^3\left(\frac{\sigma{-}1}{\sigma^2}\right)[\sigma(\gamma_1{-}\alpha) + \lambda_b Pr]z^2 \tag{2.33}$$

Therefore, accurate to O(δ), the flame stand-off distance is given by

$$d = \frac{\sigma}{\epsilon(\sqrt{\sigma}+1)} + \delta\left\{\frac{2\sigma{-}\sqrt{\sigma}{-}1}{\sqrt{\sigma}{+}1}\gamma_1 - \frac{\sqrt{\sigma}{-}1}{\sqrt{\sigma}{+}1}\lambda_b Pr - \frac{2\sigma}{\sqrt{\sigma}{+}1}\alpha\right\} \tag{2.34}$$

Further, from the definition of the flame speed (equation (1.4)), it can be shown that $a_0 = d_0 - \dfrac{1}{2\epsilon}$ and $a_1 = d_1 + \alpha$. This results in the following expression for a:

$$a = \frac{\sigma}{\epsilon(\sqrt{\sigma}{+}1)} - \frac{1}{2\epsilon} + \delta\left\{\frac{2\sigma{-}\sqrt{\sigma}{-}1}{\sqrt{\sigma}{+}1}\gamma_1 - \frac{\sqrt{\sigma}{-}1}{\sqrt{\sigma}{+}1}\lambda_b Pr + \left(1 - \frac{2\sigma}{\sqrt{\sigma}{+}1}\right)\alpha\right\} \tag{2.35}$$

Having obtained the function $F(z)$, the stream function Ψ can be evaluated and plugged in equations (2.27) through (2.29) to solve for the flow variables on the burned side of the flame. The equations (2.36), (2.37) and (2.38) below give the expressions for the axial velocity (u), transverse velocity (v) and vorticity (ω) in the outer flow field that are accurate to O(δ). They are piecewise functions that have a discontinuity or jump at the flame stand-off location $z{=}{-}d$.

$$u(z) = \begin{cases} -2\epsilon(z+a) & z < -d \\ -\dfrac{\sigma{-}1}{\sigma}\epsilon^2 z^2 - 2\epsilon\sqrt{\sigma}z + 2\epsilon^3\delta\left\{\dfrac{\sigma{-}1}{\sigma^2}\left[\sigma(\gamma_1{-}\alpha) + \lambda_b Pr\right]z^2\right\} & z > -d \end{cases} \tag{2.36}$$

$$v(z,r) = \begin{cases} \epsilon r & z < -d \\ \dfrac{\sigma-1}{\sigma}\epsilon^2 zr + \epsilon\sqrt{\sigma}r - 2\epsilon^3\delta\left\{\dfrac{\sigma-1}{\sigma^2}\Big[\sigma(\gamma_1-\alpha)+\lambda_b Pr\Big]zr\right\} & z > -d \end{cases} \tag{2.37}$$

$$\omega(r) = \begin{cases} 0 & z < -d \\ \dfrac{\sigma-1}{\sigma}\epsilon^2 r - 2\epsilon^3\delta\left\{\dfrac{\sigma-1}{\sigma^2}\Big[\sigma(\gamma_1-\alpha)+\lambda_b Pr\Big]r\right\} & z > -d \end{cases} \tag{2.38}$$

Multiplying the piecewise-constant density with the axial velocity gives an expression for the normal mass flux.

$$m(z) = \begin{cases} -2\epsilon(z+a) & z < -d \\ -\dfrac{\sigma-1}{\sigma^2}\epsilon^2 z^2 - \dfrac{2\epsilon}{\sqrt{\sigma}}z + 2\epsilon^3\delta\left\{\dfrac{\sigma-1}{\sigma^3}\Big[\sigma(\gamma_1-\alpha)+\lambda_b Pr\Big]z^2\right\} & z > -d \end{cases} \tag{2.39}$$

Having obtained the outer flow field expressions for the flow variables, it is now useful to present some of the results through plots. Several plots of the normal velocity and mass flux have been presented below in order to draw important conclusions and results. All of the plots below have been produced by simplifying equations (2.36) and (2.39) above by considering the case of constant transport properties. Similar plots can easily be generated for general cases where $\lambda = \lambda(\theta)$.

Figure 2.2 shows the variation of the leading order axial velocity along the axial direction (z). It can be seen from the figure that, as expected from equation (2.16), the leading order axial velocity (u_0) does suffer a jump of $\sigma-1$ across the flame sheet. This jump occurs at the flame sheet position or flame stand-off distance (d_0). It can also be seen that with increasing values of σ, the axial velocity on the burned side of the flame sheet and the leading order flame standoff distance d_0 increase. Lastly, it can be seen that the normal velocity becomes zero at the location $z = 0$ which corresponds to the position of the object causing the stagnation.

It is important to note that all the variables must be perturbed to the same order in order for asymptotic expressions to be consistent. For example, if the axial velocity u needs to be evaluated accurate to $\mathrm{O}(\delta)$, then all other variables including T, ρ, d, a etc. need to be perturbed to $\mathrm{O}(\delta)$ as well.

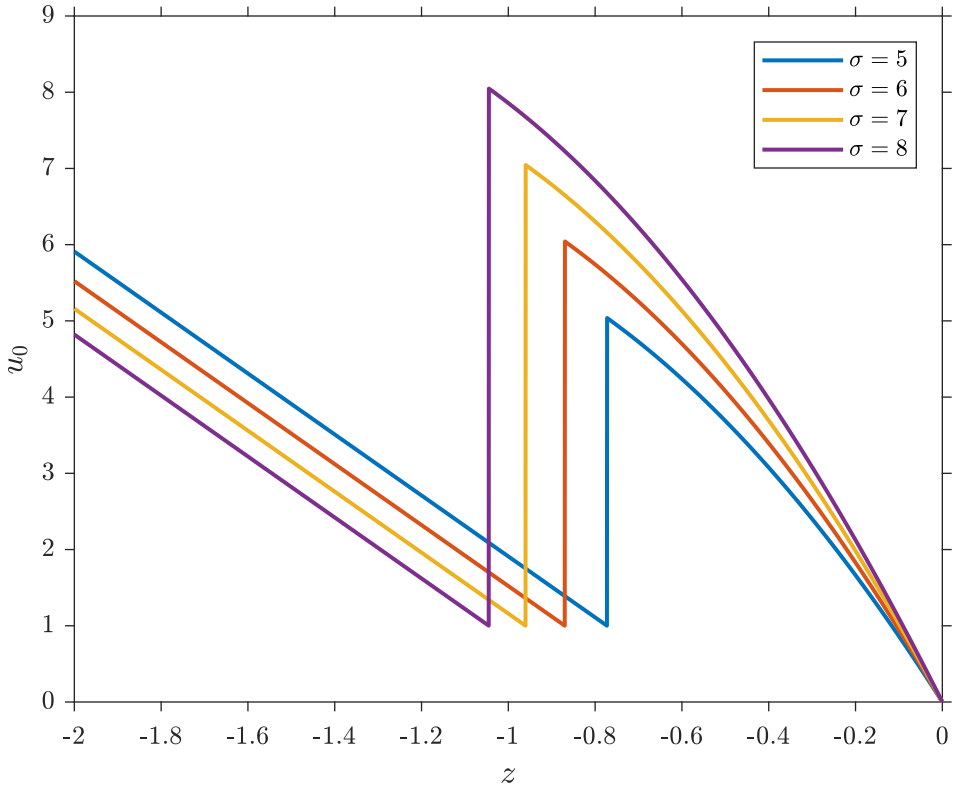

Figure 2.2: Leading order outer axial velocity (u_0) for different values of σ

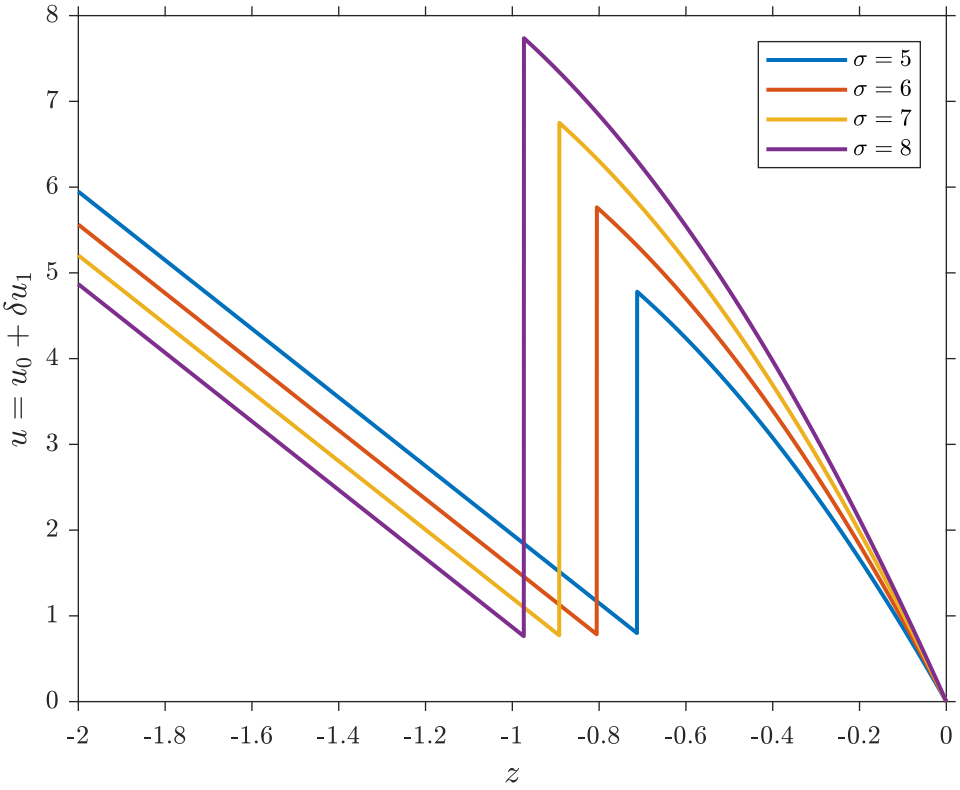

Figure 2.3: Outer axial velocity (u) accurate to O(δ) for different values of σ, and $l=0$

Figure 2.3 is similar to Figure 2.2 except that it plots the axial velocity (u) accurate to O(δ). The curves in Figure 2.3 were plotted using a value of '0' for the parameter l which measures the deviation of the effective Lewis number from unity[3]. In this case, the O(δ) terms in equation (2.36) serve as a correction to the jump in the quantity across the flame sheet. The jump in u is slightly smaller than $\sigma-1$ and the flame stand-off distance ($d=d_0+\delta d_1$) is also slightly smaller than d_0. The correlation between the thermal expansion parameter and the jump and stand-off distance remain the same as that for the leading order solution. The contrast between the leading order and O(δ) accurate axial velocity can be more explicitly seen in Figure 2.4.

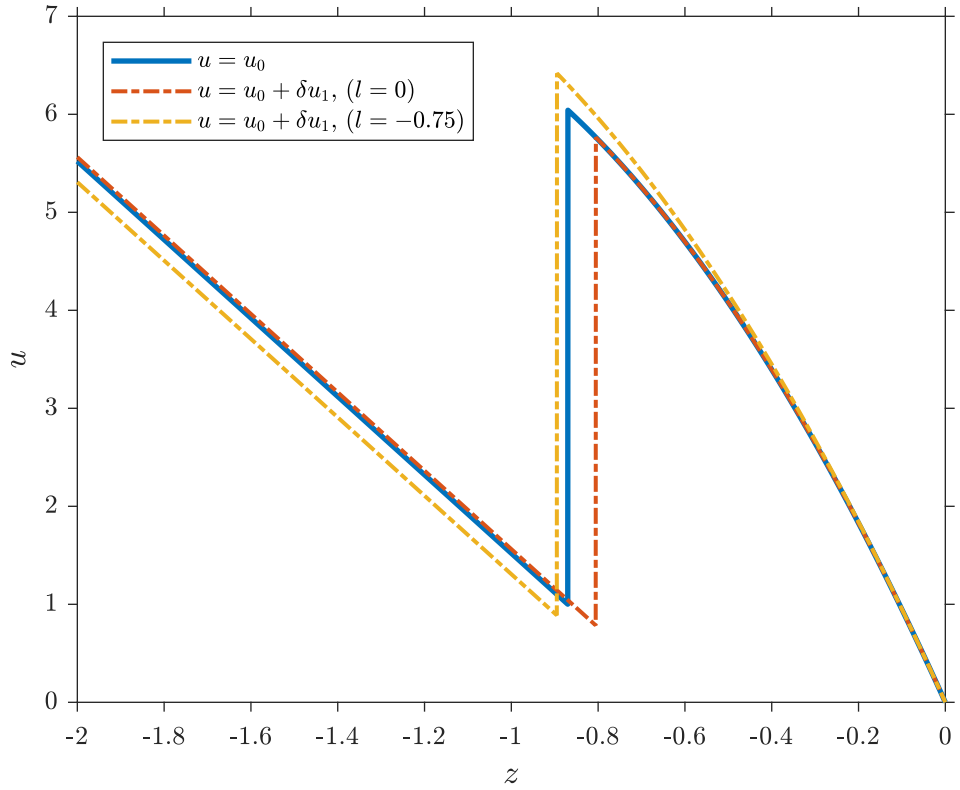

Figure 2.4: Outer axial velocities u_0 and u for different values of l, and $\sigma = 6$

Figure 2.4 compares the flame stand-off distance and jump in axial velocity accurate to O(1) and accurate to O(δ). The plot also shows that the O(δ) flame-standoff distance changes with the effective Lewis number or the parameter l. From the definition of the non-dimensional Markstein length parameter, α, given in the section 3.1, it can be seen that the Lewis number deviation parameter (l) affects its value. It has already been discussed that $\mathcal{L}$ and α change sign near $Le_{eff} = 1$. The critical value of α, and thereby l, where d_1 becomes zero can be found using

[3] l measures the deviation of Le_{eff} from unity and has been defined in sections 3.1.

equation (2.32). For the current case ($\lambda = 1$ and $\sigma = 6$), the critical value is found to be $l \approx -0.54$. For l values more negative than this critical value, the flame-standoff position shifts further to the left. In addition, as seen from the figure, the jump in velocity across the flame also sees an increase due to the change in α with l.

Figure 2.5 below contrasts the leading order and O(δ) accurate normal mass fluxes m_0 and m respectively. As suggested by the jump condition (2.9), m_0 is continuous across the flame sheet whereas m, the normal mass flux accurate to O(δ), suffers a jump because of the failure to account for lateral fluxes and accumulation at the hydrodynamic level. Additionally, it can be seen that the flame-standoff distance increases and the jump in mass flux decreases with more negative values of l.

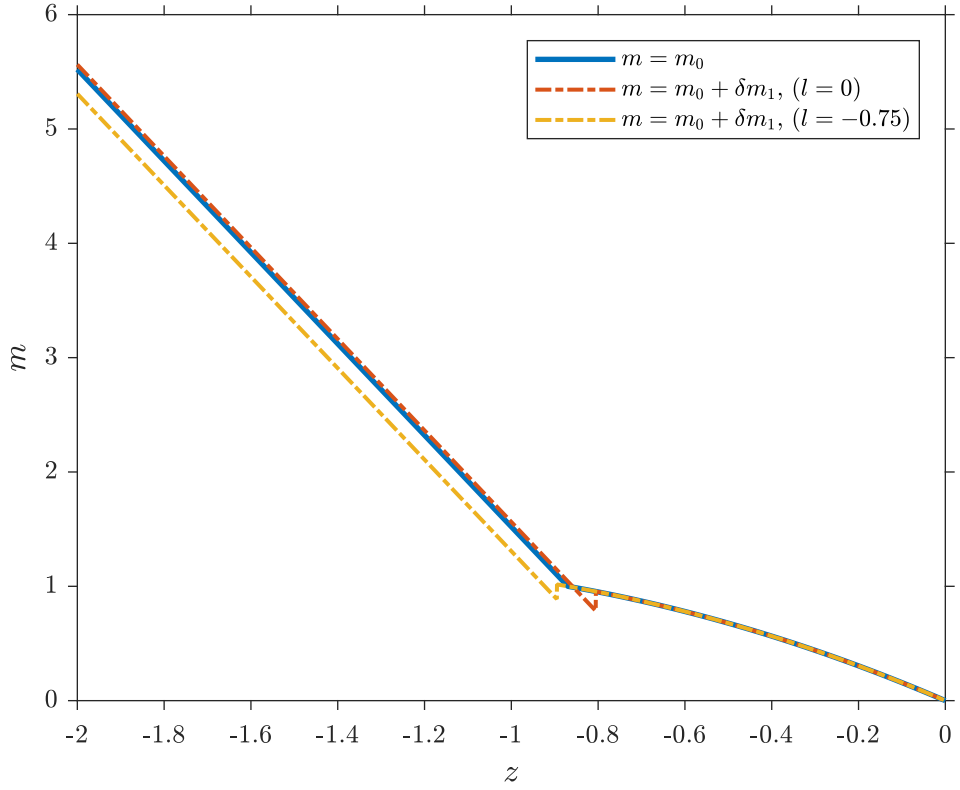

Figure 2.5: Outer normal mass fluxes m_0 and m for different values of l, and $\sigma = 6$

The flow field on the unburned side of the flame is inviscid and incompressible. Therefore, Bernoulli equation can be used to solve for the pressure field with one of the points being a virtual stagnation point (p_{vs}) corresponding to the location $z = -a_0$, $r = 0$ and the other being any location in the unburned flow field. This results in the following expression for pressure on the unburned side.

$$p(z,r) = p_{vs} - \frac{1}{2}\epsilon^2 r^2 - 2\epsilon^2(z+a_0)^2 - \delta\left\{4\epsilon^2 a_1(z+a_0)\right\} \tag{2.40}$$

Similarly, having obtained expressions for velocities on the burned side, the Navier-Stokes equations can be used to determine the pressure field. To leading order, the flow is still inviscid, and therefore, Bernoulli equation can also be used to obtain the leading order pressure term on the burned side, p_0.

$$p_0(z,r) = p_s - \frac{2}{\sigma}\left[\frac{\epsilon^2}{2}\left(\frac{\sigma-1}{\sigma}\right)z^2 + \epsilon\sqrt{\sigma}z\right]^2 - \frac{1}{2}\epsilon^2 r^2 \tag{2.41}$$

where p_s is the pressure at the stagnation point corresponding to $z=0$, $r=0$. The virtual stagnation point pressure (p_{vs}) can be related to the actual stagnation point pressure (p_s) by the jump relation (2.20).

$$p_s = p_{vs} - \frac{\sigma-1}{2} \tag{2.42}$$

However, since the viscous terms materialize as O(δ) terms, the O(δ) terms from the Navier-Stokes equations in the axial and radial directions need to be used to determine p_1 on the burned side of the flame. The O(δ) axial momentum equation is:

$$\rho u_0\frac{\partial u_1}{\partial z} + \rho u_1\frac{\partial u_0}{\partial z} = -\frac{\partial p_1}{\partial z} + Pr\left\{\frac{\partial^2 u_0}{\partial z^2} + \frac{1}{r}\frac{\partial}{\partial r}\left(r\frac{\partial u_0}{\partial r}\right)\right\}$$

Solving this gives a solution for pressure of the form

$$p_1(z,r) = \left[2\epsilon^5\frac{(\sigma-1)^2}{\sigma^4}z^4 + 4\epsilon^4\frac{(\sigma-1)}{\sigma^2\sqrt{\sigma}}z^3\right]\left[\sigma(\gamma_1-\alpha) + \lambda_b Pr\right] - 2Pr\left[\frac{\sigma-1}{\sigma}\epsilon^2 z + \epsilon\sqrt{\sigma}\right] + c_1(r) + c_2$$

where $c_1(r)$ is determined from the O(δ) radial momentum equation and the constant c_2 is determined from the boundary condition $p_1(0,0) = 0$. The O(δ) radial momentum equation is:

$$\rho u_0\frac{\partial v_1}{\partial z} + \rho u_1\frac{\partial v_0}{\partial z} + \rho v_0\frac{\partial v_1}{\partial r} + \rho v_1\frac{\partial v_0}{\partial r} = -\frac{\partial p_1}{\partial r} + Pr\left\{\frac{\partial^2 v_0}{\partial z^2} - \frac{v_0}{r^2} + \frac{1}{r}\frac{\partial v_0}{\partial r}\right\}$$

Plugging in the above mentioned expression for p_1 and solving the momentum equation using the boundary condition gives $c_1(r)=0$ and $c_2=2Pr[\epsilon\sqrt{\sigma}]$. Therefore, the O($\delta$) pressure term is only a function of the axial coordinate z and is evaluated as

$$p_1(z,r) = \left[2\epsilon^5\frac{(\sigma-1)^2}{\sigma^4}z^4 + 4\epsilon^4\frac{(\sigma-1)}{\sigma^2\sqrt{\sigma}}z^3\right]\left[\sigma(\gamma_1-\alpha) + \lambda_b Pr\right] - 2Pr\left[\frac{\sigma-1}{\sigma}\epsilon^2 z\right] \tag{2.43}$$

Chapter 3

INNER SOLUTION

This chapter presents a solution for flow variables that is valid in the inner zone or flame zone. As seen from Figure 1.1, the flame zone or thermo-diffusive zone is associated with a length scale that is much smaller in magnitude than the hydrodynamic length scale. In order to account for the mass accumulation and flame stretch effects, the coordinate z must be rescaled accounting for the diffusion of the reactants. Further, the inner pre-heat zone coordinate must be such that the reaction layer thickness l_r which is inversely proportional to the activation energy parameter (β) is much smaller than unity. In the limit $\frac{1}{\beta} \to 0$, the reaction zone shrinks to a reaction sheet and the chemical kinetics can be neglected.

In order to study the inner structure of the flame, a general first order, 2-species reaction of the following form is considered [11].

$$\nu_D \mathcal{M}_D + \nu_E \mathcal{M}_E \to PRODUCTS$$

where ν_i represents the stoichiometric coefficients, $\mathcal{M}_i$ represents the reactant species and the subscripts D and E are used to represent the deficient and excess reactants respectively. It is assumed that the deficient reactant is completely consumed across the flame. This allows the use of the transport properties of the deficient reactant as the limiting variable to the chemical reaction and heat release. The reactant mixture is stoichiometric when the two reactants are in molar proportions that lead to complete combustion; however, this may not always be the case. Therefore, a quantity Φ is introduced as the ratio of the mass fractions of the excess reactant and deficient reactant in the unburned mixture.

$$\Phi = \frac{Y_{E_u}}{\nu Y_{D_u}}$$

where $\nu = \dfrac{\nu_E W_E}{\nu_D W_D}$ is the mass-weighted stoichiometric coefficient-ratio and W_i is the mass of

reactant i. Since there are two reactants ($\mathcal{M}_D$ and $\mathcal{M}_E$), it is necessary to define an effective Lewis number (Le_{eff}) that is weighted more heavily with respect to the deficient component[1].

$$Le_{eff} = \frac{Le_E + \mathcal{A}Le_D}{\mathcal{A}+1} \tag{3.1}$$

where the weight factor $\mathcal{A} = 1 + \beta(\Phi - 1)$. In general, the properties are averaged in the reactant mixture based on mass fractions so that the average mixture thermal conductivity, $\lambda = \sum Y_i\lambda_i$, and the average mixture viscosity, $\mu = \sum Y_i\mu_i$. The only exception is the molecular diffusivity ($\mathcal{D}_i$) of the reactants, which is considered separately for each species in the reactant mixture. It has been shown that the transport properties mentioned above are, typically, functions of temperature (T), and it is assumed that the Prandtl number (Pr), Schmidt numbers (Sc_i) and Lewis numbers (Le_i) are constant. Therefore the following expression is valid for these properties:

$$\lambda = \mu = \mathcal{D}_i = \lambda(\theta) = \theta^b \tag{3.2}$$

where $\theta = \dfrac{\tilde{T}}{\tilde{T}_u}$ is the leading order non-dimensional temperature, and b is a number such that $0 < b < 1$.

In order to examine the structure of the pre-heat/flame zone, a coordinate stretching transformation has to be introduced [11]. This transformation should also incorporate the variation in transport properties that occurs across the flame or pre-heat zone. As suggested by reference [11], an inner coordinate (η) is defined as

$$\eta = \int_0^{n/\delta} \frac{1}{\lambda(n')} dn' \tag{3.3}$$

where n is the outer coordinate in the normal direction which is positive on the burned side and negative on the unburned side. The inverse transformation for (3.3) can be expressed as

$$n = \begin{cases} \delta \displaystyle\int_0^{\eta} \lambda(\eta')d\eta' & \eta < 0 \\ \\ \delta\lambda_b\eta & \eta > 0 \end{cases} \tag{3.4}$$

[1] l, defined in section 3.1, measures the deviation of Le_{eff} from unity on the scale of the inverse activation energy [10]

From equation (3.4), it can be seen that the reaction sheet is located at $\eta = 0$ with unburned gas at locations where $\eta < 0$ and burned gas at locations where $\eta > 0$. Further, the co-ordinate stretching on the burned side is uniform and does not really serve any meaningful purpose for the analysis of the pre-heat zone which is on the unburned side of the reaction sheet. The leading order non-dimensional temperature (T_0 or θ) is expressed as [9]:

$$\theta = T_0 = 1 + (\sigma - 1)e^{\eta} \tag{3.5}$$

Since $\lambda = \lambda(\theta)$, it follows that the transformation (3.3) has an implicit dependence on η. Depending on the the value of the exponent b in equation (3.2) the inner variable will be stretched to different extents as shown in Figure 3.1 below. The inner coordinate is stretched the most when λ is a constant and the least when $\lambda = \theta$.

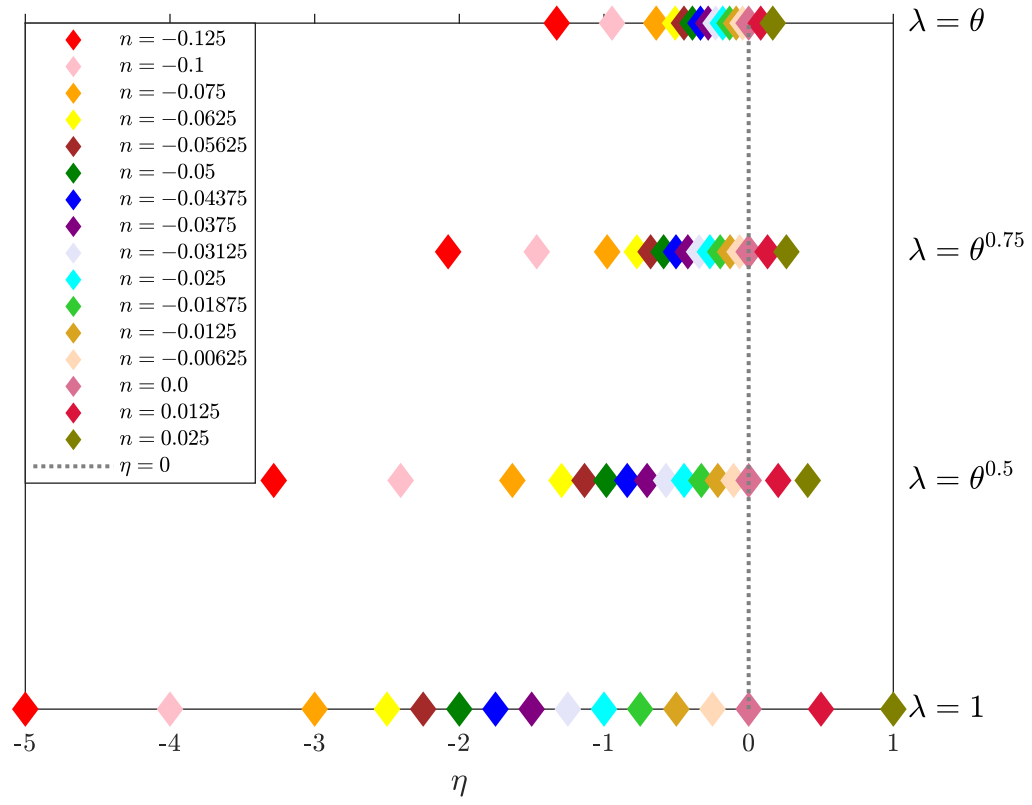

Figure 3.1: Inner coordinate η for various values of exponent b, $\delta = 0.025$ and $\sigma = 6$

3.1 DEFINITION OF INNER VARIABLES

There are several variables that appear in the inner solution; this section will define them. Lewis number is defined as the ratio of the thermal diffusivity to molecular diffusivity and is dependent on the properties of the reactants.

$$Le_i = \frac{\mathcal{D}_{th}}{\mathcal{D}_i}$$

where $\mathcal{D}_{th}$ is the thermal diffusivity of the mixture, and $\mathcal{D}_i$ is the molecular diffusivity of reactant i. The Markstein length ($\mathcal{L}$), and (its non-dimensional form $\delta\alpha$) depend on the effective Lewis number of the mixture and its proximity to unity. A parameter l measures the deviation of the effective Lewis number Le_{eff} from unity on the scale of inverse activation energy (E_a) using Zel'dovich number (β) - the parameter dictating the thickness of the reaction zone [10]. That is,

$$l = \frac{\beta(Le_{eff} - 1)}{\sigma - 1}$$

The inverse coordinate transformation from the inner coordinate (η) to the outer coordinate (n), equation (3.3), can be expressed conveniently through an integral that factors in the variation of transport properties of the reactant mixture across the flame. This integral can be evaluated as

$$I(\eta) = \int_0^\eta \lambda d\eta$$

Applying a transformation using the definition of θ, it results that

$$\eta = \ln\left(\frac{\theta - 1}{\sigma - 1}\right)$$

Using this transformation, the intergral $I(\eta)$ can be expressed as

$$I(\eta) = -\int_\theta^\sigma \frac{\lambda(x)}{x - 1} dx \tag{3.6}$$

There are several other integrals that appear in the inner expressions for mass flux, temperature and axial velocity. The expressions for these integrals are obtained by solving the rescaled governing equations (continuity, momentum and energy) in the flame zone. Firstly, $J(\eta)$ is an integral that

depends on the variation of transport coefficients within the flame zone, and it is expressed as:

$$J(\eta) = \int_0^{\eta} \rho_0 \lambda d\eta$$

By manipulating the limits of integration, $J(\eta)$ can be conveniently expressed in the following form which involves the inverse coordinate transformation integral $I(\eta)$.

$$J(\eta) = -\int_{\theta}^{\sigma} \frac{\lambda(x)}{x(x-1)} dx = \frac{\sigma - 1}{\sigma}\gamma_1 + I(\eta) - \int_1^{\theta} \frac{\lambda(x)}{x} dx \tag{3.7}$$

γ_1 and γ_2 are definite integrals that result from the flame-zone equations and are defined as:

$$\gamma_1 = \frac{\sigma}{\sigma - 1}\int_1^{\sigma} \frac{\lambda(x)}{x} dx$$

$$\gamma_2 = \int_1^{\sigma} \frac{\lambda(x)}{x} \ln\left(\frac{\sigma - 1}{x - 1}\right) dx$$

The parameter (α) depends on the effective Lewis number and the definite integrals γ_1 and γ_2 defined above, and it is defined as:

$$\alpha = \gamma_1 + \frac{l}{2}\gamma_2 \tag{3.8}$$

The non-dimensional Markstein lengths on the unburned and burned sides are respectively defined as [1]:

$$\mathcal{L}^u = \delta\alpha \tag{3.9}$$

$$\mathcal{L}^b = \delta\left\{\alpha - \int_1^{\sigma} \frac{\lambda(x)}{x} dx\right\} \tag{3.10}$$

From equation (3.8), it can be seen that there is a critical value of l for which α changes signs. As described in the introduction section, α, and consequently $\mathcal{L}$ change sign near $Le_{eff} = 1$. An indefinite integral $\chi_2(\eta)$ appears in the expression for T_1 - the O(δ) temperature term, and it is defined as:

$$\chi_2(\eta) = \int_{\eta}^{0} \left(\kappa I(\eta') - \mathbb{K}J(\eta') + \lambda\kappa\right)\left(e^{\eta'} - e^{\eta}\right) d\eta'$$

Since the flow under consideration is a stagnation point flow, the curvature, $\kappa=0$. Plugging in this simplification and factoring out $\mathbb{K}$ gives

$$\tilde{\chi}_2(\eta) = \frac{\chi_2(\eta)}{\mathbb{K}} = \int_{\eta}^{0} J(\eta')\left(e^{\eta} - e^{\eta'}\right)d\eta'$$

When the transport properties are constant ($\lambda=1$), the expressions for definite integrals γ_1 and γ_2 can be simplified. This gives the following expressions for γ_1 and α.

$$\widetilde{\gamma}_1 = \frac{\sigma \ln \sigma}{\sigma - 1}$$

$$\alpha = \widetilde{\gamma}_1 + \frac{l}{2}\int_{1}^{\sigma} \frac{\ln s}{s-1} ds$$

Additionally, for the case with constant transport properties, $I(\eta)=\eta$.

3.2 GENERAL SOLUTION

The results for mass flux and temperature presented in this section have been obtained from the paper by Matalon and Bechtold [11]. The expressions given in the paper have been simplified for an adiabatic flame. The expressions presented below for all the inner variables are piecewise functions as expected from the fact that temperature varies across the pre-heat zone but is a constant on the burned side of the adiabatic flame. The inner/flame-zone expression for the normal mass flux across the flame accurate to $\mathrm{O}(\delta)$ is

$$M(\eta) = \begin{cases} 1 + \delta\left\{\mathbb{K}\left[\dfrac{\sigma-1}{\sigma}\gamma_1 - \alpha - J(\eta)\right] + \kappa I(\eta)\right\} & \eta < 0 \\ 1 + \delta\left\{\mathbb{K}\left[\dfrac{\sigma-1}{\sigma}\gamma_1 - \alpha - \dfrac{\eta\lambda_b}{\sigma}\right] + \kappa\eta\lambda_b\right\} & \eta > 0 \end{cases} \tag{3.11}$$

where $I(\eta)$ and $J(\eta)$ are integrals defined in section 3.1. It can be seen that the equation (3.11) contains correction terms of $\mathrm{O}(\delta)$ that account for the flame stretch due to hydrodynamic strain

and curvature. The expression for temperature accurate to O(δ) is

$$T(\eta) = \begin{cases} \theta + \delta\left\{(\sigma-1)\mathbb{K}\left[\dfrac{\sigma-1}{\sigma}\gamma_1\eta e^{\eta} - \alpha\eta e^{\eta} + \dfrac{\gamma_1}{\sigma}(e^{\eta}-1)\right] + (\sigma-1)\chi_2(\eta)\right\} & \eta < 0 \\ \sigma & \eta > 0 \end{cases} \tag{3.12}$$

where $\theta = 1 + (\sigma - 1)e^{\eta}$ as defined before and $\chi_2(\eta)$ is an indefinite integral defined in section 3.1. From the ideal gas law in non-dimensional form, it follows that $\rho T = 1$. Using equation (3.12) in the ideal gas law and using the binomial expansion: $(A_0 + \delta A_1)^{-1} \approx A_0 - \delta A_1$ gives a piecewise expression for density that is valid to O(δ).

$$\rho(\eta) = \begin{cases} \dfrac{1}{\theta} - \delta\left\{\dfrac{(\sigma-1)\mathbb{K}\left[\dfrac{\sigma-1}{\sigma}\gamma_1\eta e^{\eta} - \alpha\eta e^{\eta} + \dfrac{\gamma_1}{\sigma}(e^{\eta}-1)\right] + (\sigma-1)\chi_2(\eta)}{1+2(\theta-1)+(\theta-1)^2}\right\} & \eta < 0 \\ \dfrac{1}{\sigma} & \eta > 0 \end{cases} \tag{3.13}$$

Using the definition of normal mass flux as the product of the density and normal gas velocity with respect to a fixed coordinate system, the following expression for the normal velocity is obtained.

$$v_n(\eta) - V_f = \begin{cases} \theta + \delta\left\{\mathbb{K}\theta\left[\dfrac{\sigma-1}{\sigma}\gamma_1 - \alpha - J(\eta)\right] + \kappa\theta I(\eta)\right. \\ \qquad \left. + (\sigma-1)\mathbb{K}\left[\dfrac{\sigma-1}{\sigma}\gamma_1\eta e^{\eta} - \alpha\eta e^{\eta} + \dfrac{\gamma_1}{\sigma}(e^{\eta}-1)\right] + (\sigma-1)\chi_2(\eta)\right\} & \eta < 0 \\ \sigma + \delta\left\{\mathbb{K}\left[(\sigma-1)\gamma_1 - \sigma\alpha - \eta\lambda_b\right] + \kappa\sigma\eta\lambda_b\right\} & \eta > 0 \end{cases} \tag{3.14}$$

3.3 SOLUTION FOR STAGNATION POINT FLOW

For the axisymmetric stagnation point flow studied, the flame is planar and is stabilized at a stand-off distance (d) from the stagnation point, i.e. $\kappa = 0$ and $V_f = 0$. Further, the flame stretch $\mathbb{K} = 2\epsilon$. Additionally, since the flame is located at $z = -d$, the normal coordinate $n = z + d$, and this leads

to the following coordinate transformation:

$$z + d = \begin{cases} \delta \int_0^{\eta} \lambda(\eta') d\eta' & \eta < 0 \\ \delta \lambda_b \eta & \eta > 0 \end{cases}$$

3.3.1 Properties Varying with Temperature ($\lambda = \lambda(\theta)$)

When the transport properties are not constant, the integrals $I(\eta)$, $J(\eta)$ and $\chi_2(\eta)$ need to be evaluated. Since these integrals are dependent on the position η in the inner coordinate system, and since the integrand λ is also changing with η, they cannot be substituted by simple expressions. Plugging the stagnation point flow simplifications into equations (3.11) through (3.14) results in the following equations for the inner variables.

$$M(\eta) = \begin{cases} 1 + 2\epsilon\delta\left\{\frac{\sigma-1}{\sigma}\gamma_1 - \alpha - J(\eta)\right\} & \eta < 0 \\ 1 + 2\epsilon\delta\left\{\frac{\sigma-1}{\sigma}\gamma_1 - \alpha - \frac{\eta\lambda_b}{\sigma}\right\} & \eta > 0 \end{cases} \tag{3.15}$$

$$T(\eta) = \begin{cases} 1 + (\sigma-1)e^{\eta} + 2\epsilon\delta\left\{(\sigma-1)\left[\frac{\sigma-1}{\sigma}\gamma_1\eta e^{\eta} - \alpha\eta e^{\eta} + \frac{\gamma_1}{\sigma}(e^{\eta}-1) + \tilde{\chi}_2(\eta)\right]\right\} & \eta < 0 \\ \sigma & \eta > 0 \end{cases} \tag{3.16}$$

$$\rho(\eta) = \begin{cases} \frac{1}{1+(\sigma-1)e^{\eta}} - 2\epsilon\delta\left\{\frac{(\sigma-1)\left[\frac{\sigma-1}{\sigma}\gamma_1\eta e^{\eta} - \alpha\eta e^{\eta} + \frac{\gamma_1}{\sigma}(e^{\eta}-1) + \tilde{\chi}_2(\eta)\right]}{1+2(\sigma-1)e^{\eta}+(\sigma-1)^2e^{2\eta}}\right\} & \eta < 0 \\ \frac{1}{\sigma} & \eta > 0 \end{cases} \tag{3.17}$$

$$U(\eta) = \begin{cases} 1 + (\sigma-1)e^{\eta} + 2\epsilon\delta\left\{\left[1 + (\sigma-1)e^{\eta}\right]\left[\frac{\sigma-1}{\sigma}\gamma_1 - \alpha - J(\eta)\right]\right. \\ \qquad \left. + (\sigma-1)\left[\frac{\sigma-1}{\sigma}\gamma_1\eta e^{\eta} - \alpha\eta e^{\eta} + \frac{\gamma_1}{\sigma}(e^{\eta}-1) + \tilde{\chi}_2(\eta)\right]\right\} & \eta < 0 \\ \sigma + 2\epsilon\delta\left\{(\sigma-1)\gamma_1 - \sigma\alpha - \eta\lambda_b\right\} & \eta > 0 \end{cases} \tag{3.18}$$

3.3.2 Constant Properties ($\lambda = 1$)

When the transport properties are constant, the integrals $I(\eta)$, $J(\eta)$ and $\chi_2(\eta)$ in equations (3.15) through (3.18) can be easily evaluated. In particular, the outer coordinate stretch becomes uniform, i.e., when $\lambda=1$, the coordinate transformation is

$$\eta = \frac{z+d}{\delta}$$

This results in the following expressions for the inner variables M, T, ρ and u respectively.

$$M(\eta) = \begin{cases} 1 + 2\epsilon\delta\left\{\ln\theta - \alpha - \eta\right\} & \eta < 0 \\ 1 + 2\epsilon\delta\left\{\ln\sigma - \alpha - \dfrac{\eta}{\sigma}\right\} & \eta > 0 \end{cases} \tag{3.19}$$

$$T(\eta) = \begin{cases} 1 + (\sigma-1)e^{\eta} + 2\epsilon\delta\left\{\left[\widetilde{\gamma}_1 + (1-\alpha)\eta - \dfrac{\eta^2}{2} - I_2(\eta)\right](\sigma-1)e^{\eta}\right. \\ \qquad \left. -\left[1+(\sigma-1)e^{\eta}\right]\ln\left(1+(\sigma-1)e^{\eta}\right)\right\} & \eta < 0 \\ \sigma & \eta > 0 \end{cases} \tag{3.20}$$

$$\rho(\eta) = \begin{cases} \dfrac{1}{1+(\sigma-1)e^{\eta}} - 2\epsilon\delta\left\{\dfrac{\left[\widetilde{\gamma}_1 + (1-\alpha)\eta - \dfrac{\eta^2}{2} - I_2(\eta)\right](\sigma-1)e^{\eta}}{1+2(\sigma-1)e^{\eta}+(\sigma-1)^2e^{2\eta}}\right. \\ \qquad \left. - \dfrac{\left[1+(\sigma-1)e^{\eta}\right]\ln\left(1+(\sigma-1)e^{\eta}\right)}{1+2(\sigma-1)e^{\eta}+(\sigma-1)^2e^{2\eta}}\right\} & \eta < 0 \\ \dfrac{1}{\sigma} & \eta > 0 \end{cases} \tag{3.21}$$

$$U(\eta) = \begin{cases} 1 + (\sigma-1)e^{\eta} + 2\epsilon\delta\left\{\left[1+(\sigma-1)e^{\eta}\right]\left[\ln\left(1+(\sigma-1)e^{\eta}\right) - \alpha - \eta\right]\right. \\ \quad \left. +\left[\widetilde{\gamma}_1 + (1-\alpha)\eta - \dfrac{\eta^2}{2} - I_2(\eta)\right](\sigma-1)e^{\eta} - \left[1+(\sigma-1)e^{\eta}\right]\ln\left(1+(\sigma-1)e^{\eta}\right)\right\} & \eta < 0 \\ \sigma + 2\epsilon\delta\left\{\sigma\ln\sigma - \sigma\alpha - \eta\right\} & \eta > 0 \end{cases} \tag{3.22}$$

where $I_2(\eta) = \displaystyle\int_{\eta}^{0} \ln\left(1+(\sigma-1)e^{\eta}\right) d\eta$.

Chapter 4

COMPOSITE SOLUTION

A composite expression for the flow variables is one that is valid in both the inner flame zone and outer hydrodynamic zone. In other words, the composite expression is valid throughout the domain of the problem, but it has a discontinuity in slope at the location of the reaction sheet. Having obtained an outer solution for the normal mass flux that is valid in the hydrodynamic unburned and burned regions (Chapter 2) and an inner solution that is valid inside the flame zone (Chapter 3), a uniformly valid composite expression for the normal mass flux can be obtained by matching the inner and outer solutions. In other words,

$$\{Composite\,Solution\} = \{Outer\,Solution\} + \{Inner\,Solution\} - \{Common\,Part\}$$

4.1 MATCHING

The inner solution should give the same result as the outer solution in the asymptotic limit where the inner coordinate η approaches a large value in both positive (burned) and negative (unburned) directions. Similarly, the outer solution should give the same result as the inner solution when the outer coordinate z approaches the flame-standoff distance d from both unburned and burned regions. In order to match the inner and outer solutions and determine the common part, the inner solution needs to be expressed in terms of the outer variable z and the outer solution needs to be expressed in terms of the inner variable η.

4.1.1 Properties Varying with Temperature ($\lambda = \lambda(\theta)$)

Equation (3.15) gives the inner (flame zone) expression for the normal mass flux. In the asymptotic limit $\eta \to -\infty$,

$$\theta \to 1 + Exponentially\ Smaller\ Terms$$

$$J(\eta) \to \frac{\sigma-1}{\sigma}\gamma_1 + I(\eta)$$

Therefore, for large η, the inner expression for mass flux becomes:

$$M \approx \begin{cases} 1 - 2\epsilon\delta\Big\{\alpha+I(\eta)\Big\} & \eta < 0 \\ 1 + 2\epsilon\delta\Big\{\dfrac{\sigma-1}{\sigma}\gamma_1-\alpha-\dfrac{\eta\lambda_b}{\sigma}\Big\} & \eta > 0 \end{cases} \tag{4.1}$$

Equation (2.39) gives the expression for the outer mass flux (m). Expressing the outer coordinate in terms of the inner coordinate gives $z=-d_0+\delta[I(\eta)-d_1]$. Substituting this in the expression for m gives

$$m \approx \begin{cases} -2\epsilon\Big[(a_0-d_0) + \delta(I(\eta)+a_1-d_1)\Big] & z < -d \\ -\dfrac{\sigma-1}{\sigma^2}\epsilon^2\Big[-d_0+\delta[I(\eta)-d_1]\Big]^2 - \dfrac{2\epsilon}{\sqrt{\sigma}}\Big[-d_0+\delta[I(\eta)-d_1]\Big] & \\ \quad +2\epsilon^3\delta\Big\{\dfrac{\sigma-1}{\sigma^3}\Big[\sigma(\gamma_1-\alpha) + \lambda_b Pr\Big]\Big[-d_0+\delta[I(\eta)-d_1]\Big]^2\Big\} & z > -d \end{cases}$$

Simplifying the above equation using expressions for d_0, d_1, (a_0-d_0) and (a_1-d_1) gives

$$m \approx \begin{cases} 1 - 2\epsilon\delta\Big\{\alpha+I(\eta)\Big\} & \eta < 0 \\ 1 + 2\epsilon\delta\Big\{\dfrac{\sigma-1}{\sigma}\gamma_1-\alpha-\dfrac{\eta\lambda_b}{\sigma}\Big\} & \eta > 0 \end{cases} \tag{4.2}$$

Comparing equations (4.1) and (4.2), it is seen that the inner and outer expressions for the mass flux indeed match. The composite expression for the normal mass flux can be obtained by adding the inner and outer solutions and subtracting the common part. The common part between the outer and inner expressions is $1 - 2\epsilon\delta[\alpha+I(\eta)]$ on the unburned side and the inner expression, $M(\eta)$, on the burned side, i.e.,

$$m_c(z) = \begin{cases} m(z) + M(\eta) - \Big\{1 - 2\epsilon\delta[\alpha+I(\eta)]\Big\} & z < -d \\ m(z) + M(\eta) - \Big\{M(\eta)\Big\} & z > -d \end{cases}$$

Evaluating this gives the following uniformly valid composite expression for the normal mass flux across the flame:

$$m_c(z) = \begin{cases} -2\epsilon(z+a) + 2\epsilon\delta\left\{\int_1^\theta \frac{\lambda(x)}{x}dx\right\} & z < -d \\ -\frac{\sigma-1}{\sigma^2}\epsilon^2 z^2 - \frac{2\epsilon}{\sqrt{\sigma}}z + 2\epsilon^3\delta\left\{\frac{\sigma-1}{\sigma^3}\left[\sigma(\gamma_1-\alpha) + \lambda_b Pr\right]z^2\right\} & z > -d \end{cases} \tag{4.3}$$

Additionally, in the limit $\eta \to -\infty$,

$$\chi_2(\eta) \to \frac{\gamma_1}{\sigma}$$

$$T_1 \to 0$$

Hence, in the limit of large η, the inner expression for the axial velocity reduces to:

$$U \approx \begin{cases} 1 - 2\epsilon\delta\left\{\alpha + I(\eta)\right\} & \eta < 0 \\ \sigma + 2\epsilon\delta\left\{(\sigma-1)\gamma_1 - \sigma\alpha - \eta\lambda_b\right\} & \eta > 0 \end{cases} \tag{4.4}$$

The outer expression for the axial velocity presented in equation (2.36) needs to be expanded in terms of the inner coordinate. Using $z = -d_0 + \delta[I(\eta) - d_1]$, it follows that

$$u \approx \begin{cases} -2\epsilon\left[(a_0 - d_0) + \delta(I(\eta) + a_1 - d_1)\right] & z < -d \\ -\frac{\sigma-1}{\sigma}\epsilon^2\left[-d_0 + \delta[I(\eta) - d_1]\right]^2 - 2\epsilon\sqrt{\sigma}\left[-d_0 + \delta[I(\eta) - d_1]\right] & \\ \quad + 2\epsilon^3\delta\left\{\frac{\sigma-1}{\sigma^2}\left[\sigma(\gamma_1-\alpha) + \lambda_b Pr\right]\left[-d_0 + \delta[I(\eta) - d_1]\right]^2\right\} & z > -d \end{cases}$$

which again can be simplified by plugging in values of d and a. This gives the following outer expression for the axial velocity.

$$u \approx \begin{cases} 1 - 2\epsilon\delta\left\{\alpha + I(\eta)\right\} & \eta < 0 \\ \sigma + 2\epsilon\delta\left\{(\sigma-1)\gamma_1 - \sigma\alpha - \eta\lambda_b\right\} & \eta > 0 \end{cases} \tag{4.5}$$

Equations (4.4) and (4.5) are identical, and so the inner and outer expressions for the axial velocity match. Following a procedure similar to the one detailed above for mass flux, a uniformly valid

expression for axial velocity can be obtained. The composite solution for u on the unburned side is of the form $u_c = -2\epsilon(z+a) + (\theta-1) + 2\epsilon\delta\left\{\theta\int_1^\theta \frac{\lambda(x)}{x}dx - (\theta-1)[I(\eta)+\alpha] + T_1\right\}$ where T_1 is the $O(\delta)$ temperature. Expanding the variables θ, η and T_1 gives

$$u_c(z) = \begin{cases} -2\epsilon(z+a) + (\sigma-1)\exp\left(\frac{z+d}{\delta}\right) + 2\epsilon\delta\left\{\left[1+(\sigma-1)\exp\left(\frac{z+d}{\delta}\right)\right]\int_1^\theta \frac{\lambda(x)}{x}dx \right. \\ \quad +(\sigma-1)\left[\frac{\gamma_1}{\sigma}\left[(\sigma-1)\frac{z+d}{\delta}\exp\left(\frac{z+d}{\delta}\right) + \exp\left(\frac{z+d}{\delta}\right) - 1\right]\right. \\ \left.\left. \qquad -\alpha\left[\exp\left(\frac{z+d}{\delta}\right)\left(1-\frac{z+d}{\delta}\right)\right] - I(z)\exp\left(\frac{z+d}{\delta}\right) + \chi_2(z)\right]\right\} & z < -d \\ -\frac{\sigma-1}{\sigma}\epsilon^2 z^2 - 2\epsilon\sqrt{\sigma}z + 2\epsilon^3\delta\left\{\frac{\sigma-1}{\sigma^2}\left[\sigma(\gamma_1-\alpha) + \lambda_b Pr\right]z^2\right\} & z > -d \end{cases} \tag{4.6}$$

Since the inner expression for axial velocity U involves the integral $\chi_2(\eta)$, a composite expression for the axial velocity is more conveniently calculated using the relation:

$$u_c = \frac{m_c}{\rho} \tag{4.7}$$

where ρ is given by equation (3.21).

4.1.2 Constant Properties ($\lambda = 1$)

In the case of constant transport properties, the integrals in the equations above can further be simplified. Since this is a special case of the problem with variable properties, the inner and outer solutions should match and this can be easily verified using a matching procedure similar to the one described in the above section. Similarly, addition of the outer and inner solutions and subtraction of the common part results in the following uniformly valid composite expressions for the normal mass flux and velocity respectively.

$$m_c(z) = \begin{cases} -2\epsilon(z+a) + 2\epsilon\delta\left\{\ln\left[1+(\sigma-1)\exp\left(\frac{z+d}{\delta}\right)\right]\right\} & z < -d \\ -\frac{\sigma-1}{\sigma^2}\epsilon^2 z^2 - \frac{2\epsilon}{\sqrt{\sigma}}z + 2\epsilon^3\delta\left\{\frac{\sigma-1}{\sigma^3}\left[\sigma(\gamma_1-\alpha) + \lambda_b Pr\right]z^2\right\} & z > -d \end{cases} \tag{4.8}$$

$$u_c(z) = \begin{cases} -2\epsilon(z+a) + (\sigma-1)\exp\left(\frac{z+d}{\delta}\right) + 2\epsilon\delta\left\{\theta\ln\theta - (\theta-1)(\eta+\alpha) + T_1\right\} & z < -d \\ -\frac{\sigma-1}{\sigma}\epsilon^2 z^2 - 2\epsilon\sqrt{\sigma}z + 2\epsilon^3\delta\left\{\frac{\sigma-1}{\sigma^2}\left[\sigma(\tilde{\gamma}_1-\alpha) + Pr\right]z^2\right\} & z > -d \end{cases} \tag{4.9}$$

4.2 RESULTS AND DISCUSSION

The results and discussion provided here are primarily for the case where the transport properties are constant across the flame. However, these results can easily be extended to the general case where the transport properties vary with temperature ($\lambda = \lambda(\theta)$).

4.2.1 Composite Profiles Across the Flame

The composite solutions for the normal mass flux and velocity across the flame, given in equations (4.8) and (4.9) respectively, are continuous in the entire domain. Figure 4.1 below plots the composite velocity, u_c, for several different values of the thermal expansion parameter. The position of the flame in these plots can be identified by the sharp positive gradients in velocity. As can be seen from the figure, the discontinuity or jump in velocity at the flame-standoff location d does not exist anymore. This is because the composite solution includes correction terms from the inner solution that account for lateral fluxes and accumulation of mass. Further, it can be seen that the flame has a small but finite thickness (δ) over which the axial velocity encounters a rapid increase in magnitude. However, it should be noted that the composite solution did not resolve the structure of the reaction zone which is an order of magnitude smaller in thickness than the flame zone. This results in a discontinuity in the slope on the burned side of the flame which can be clearly seen in the plots. The resolution of this disparity in slope requires another rescale of the coordinate using the Zeldovich number (β) and does not significantly affect the solution except for matching the slope on the burned side of the flame.

Figure 4.2 depicts the variation of temperature across the flame for different values of the thermal expansion parameter σ. As expected, the non-dimensional temperature (T) is unity far upstream of the flame and σ on the burned side of the flame. Additionally, as seen from the outer solution presented in section 3.3, the flame-standoff distance increases in magnitude with increasing values of σ. Similar to the axial velocity profiles in Figure 4.1, the temperature profiles also have a discontinuity in slope at the reaction sheet location because chemical kinetics in the reaction zone were ignored. Resolving the structure of the reaction zone would fix this discontinuity of slope, but since the quantity of interest is temperature, and not the gradient of temperature, the resolution of the reaction zone structure is not necessary for the problem studied.

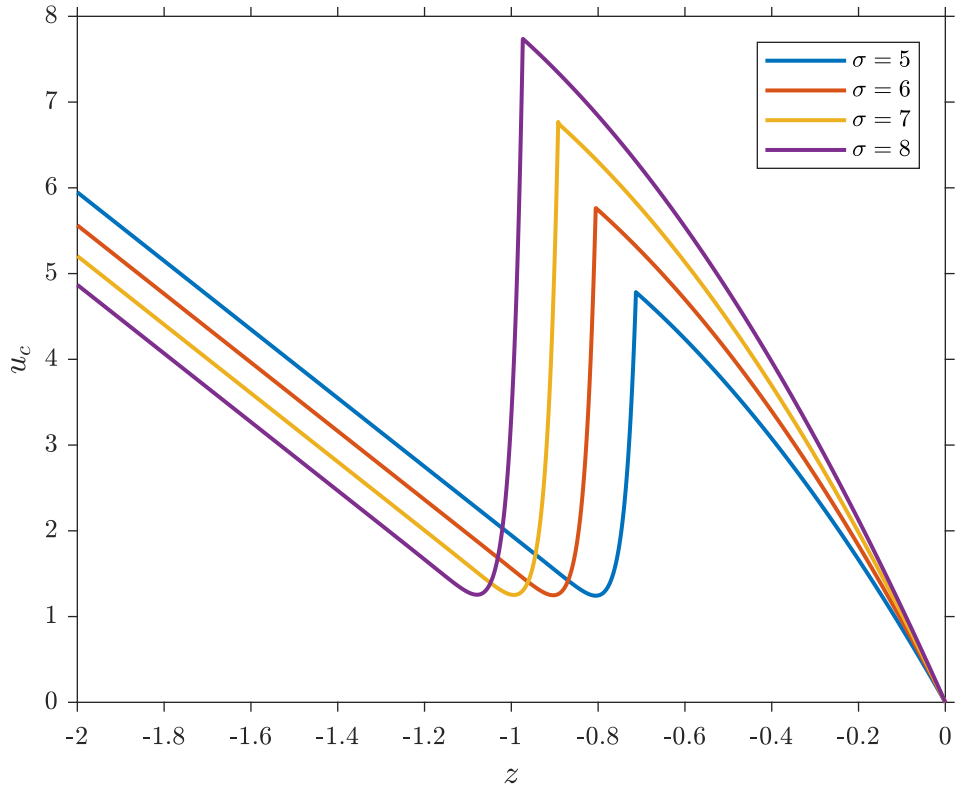

Figure 4.1: Composite axial velocity u_c for different values of σ, and $\delta = 0.025$

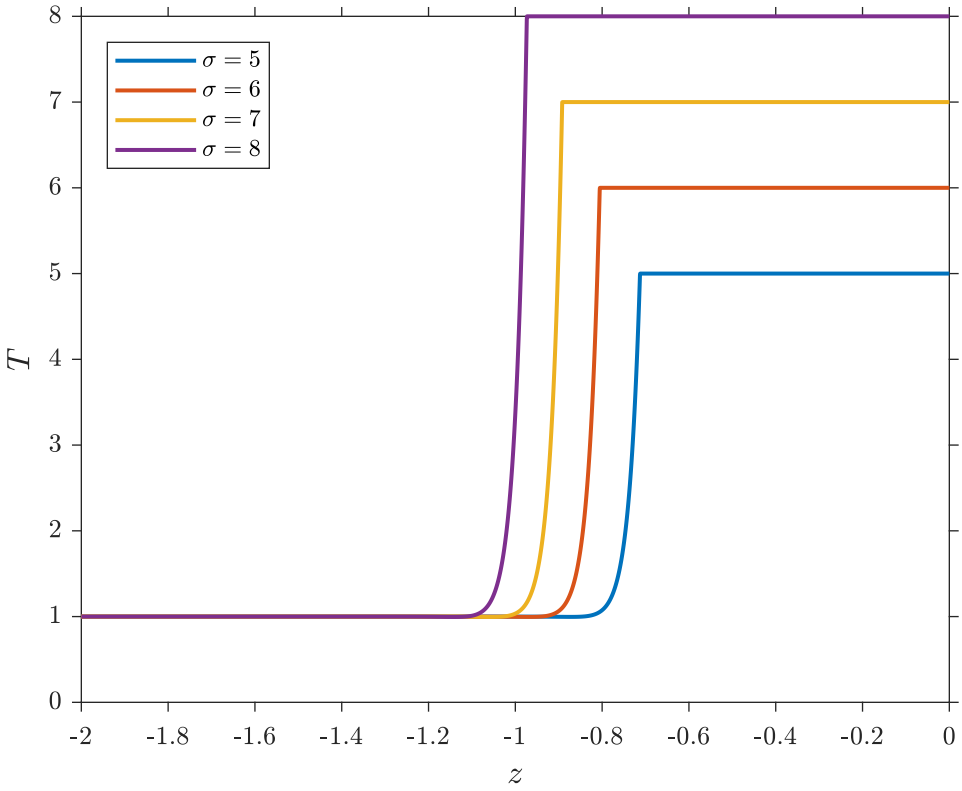

Figure 4.2: Temperature profiles across the flame for different values of σ, and $\delta = 0.025$

Since the composite axial velocity can be calculated either as m_c/ρ or using equation (4.9), a comparison can be made between the two. Figure 4.3 below shows that the two curves practically lie on top of each other. Specifically, equations (4.7) and (4.9) yield very similar solutions proving that the composite expression for u_c given in equation (4.9) is indeed accurate.

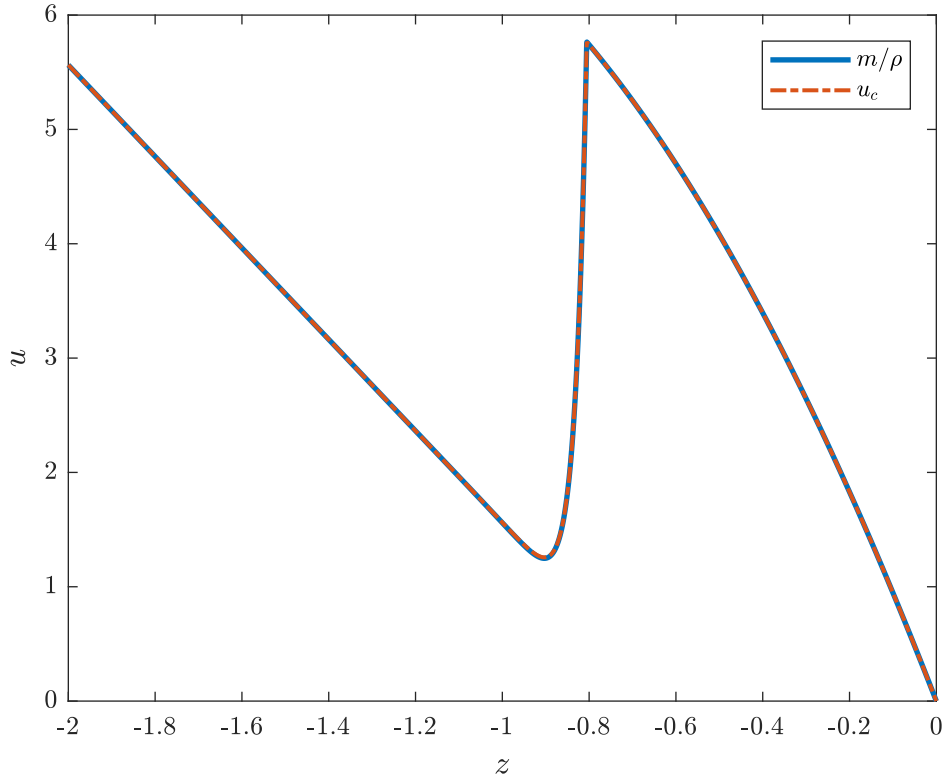

Figure 4.3: Comparison of u_c calculated using two methods, for $\sigma = 6$ and $\delta = 0.025$

4.2.2 Markstein Length and Flame Displacement Speed Within the Flame Zone

Having obtained the composite expression for the normal gas velocity and mass flux, the flame displacement speed defined in equation (1.1) can now be evaluated as:

$$S_f = u_c|_{z=-d^-} = \left.\frac{m_c}{\rho}\right|_{z=-d^-}$$

This expression is unique only in the hydrodynamic sense where the entire flame zone reduces to a surface known as the flame sheet which is located at the position $z = -d$. In reality, the flame has a finite thickness (δ), and so, the expression for flame displacement speed needs to account for the O(δ) position within the flame zone. This means that a position or isotherm within the flame

zone (where velocity is measured) would not be at $z^* = -d$, instead it will be at $z^* = -d + \delta I(\eta)$. Therefore, the correct evaluation of the flame displacement speed would account for the flame thickness and, for a location z^*, is given by:

$$S_f^* = u_c|_{z^*=-d+\delta I(\eta)} = \frac{m_c}{\rho}\bigg|_{z^*=-d+\delta I(\eta)} \tag{4.10}$$

Since the density also changes throughout the flame zone from its unburned value of unity, the flame displacement speed at any position within the flame zone is normalized using the ratio of the density at that location (ρ^*) and the density on the unburned side ($\rho_u = 1$). The density-weighted flame displacement speed is defined as

$$\tilde{S_f^*} = \frac{\rho^* S_f^*}{\rho_u} = m_c\bigg|_{z^*=-d+\delta I(\eta)} \tag{4.11}$$

and can be used to meaningfully compare the flame speed evaluated at different locations within the flame. Using equation (4.11), the density-weighted flame displacement speed can be evaluated at any location within the flame. Using equation (4.3) for the normal mass flux,

$$\tilde{S_f^*} = -2\epsilon\Big[a - d + \delta I(\eta)\Big] + 2\epsilon\delta\left\{\int_1^{\theta^*} \frac{\lambda(x)}{x} dx\right\}$$

which can further be simplified using the relation between a and d.

For $\lambda = \lambda(\theta)$:

$$\tilde{S_f^*} = 1 - 2\epsilon\delta\left\{\alpha - \int_1^{\theta^*} \frac{\lambda(x)}{x} dx - \int_{\theta^*}^{\sigma} \frac{\lambda(x)}{x-1} dx\right\} \tag{4.12}$$

which is of the form $\tilde{S_f^*} = 1 - 2\epsilon\mathcal{L}^*$ where

$$\mathcal{L}^* = \delta\alpha^* = \delta\left\{\alpha - \int_1^{\theta^*} \frac{\lambda(x)}{x} dx - \int_{\theta^*}^{\sigma} \frac{\lambda(x)}{x-1} dx\right\} \tag{4.13}$$

For $\lambda = 1$:

$$\tilde{S_f^*} = 1 - 2\epsilon\delta\left\{\alpha + \eta - \ln\Big(1 + (\sigma - 1)e^{\eta}\Big)\right\} \tag{4.14}$$

which again is of the form $\tilde{S}_f^* = 1 - 2\epsilon\mathcal{L}^*$ where

$$\mathcal{L}^* = \delta\alpha^* = \delta\left\{\alpha + \eta - \ln\left(1 + (\sigma - 1)e^{\eta}\right)\right\} \tag{4.15}$$

From the above expressions for the non-dimensional Markstein length within the flame zone ($\mathcal{L}^*$), it can be seen that the expression for $\mathcal{L}^b$ is regained at the location of the reaction sheet where $\theta^* = \sigma$. On the other hand, when $\theta^* \approx 1$, the Markstein length becomes a large negative number. This trend can be clearly seen in Figure 4.4 which shows the variation of Markstein number, $\mathcal{M} = \dfrac{\mathcal{L}}{\delta}$, with temperature.

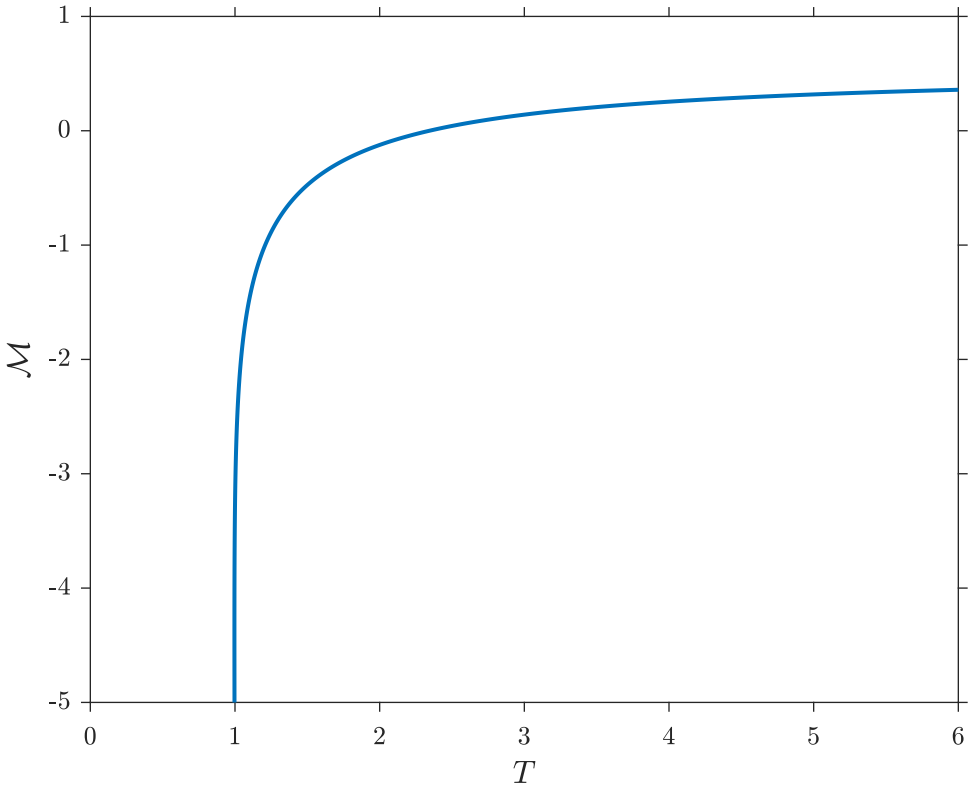

Figure 4.4: Markstein number $\mathcal{M}$ as a function of temperature

Figure 4.5 below shows the variation of normal velocity, mass flux and temperature across a flame. All three variables are continuous across the flame, and the normal velocity and mass flux go to zero at the wall/stagnation point. In particular, the discontinuity in mass flux no longer exists due to accountancy of the effects of lateral fluxes due to flame stretch. Figure 4.5 also includes an inset showing the profiles in the flame zone. From the inset, it can be seen that the temperature is significantly higher than the unburned temperature (T_u) at the location of the minimum velocity

($\bar{z}$). In fact, for the parameters used for the plot, $T(\bar{z}) = \bar{T} \approx 1.1$.

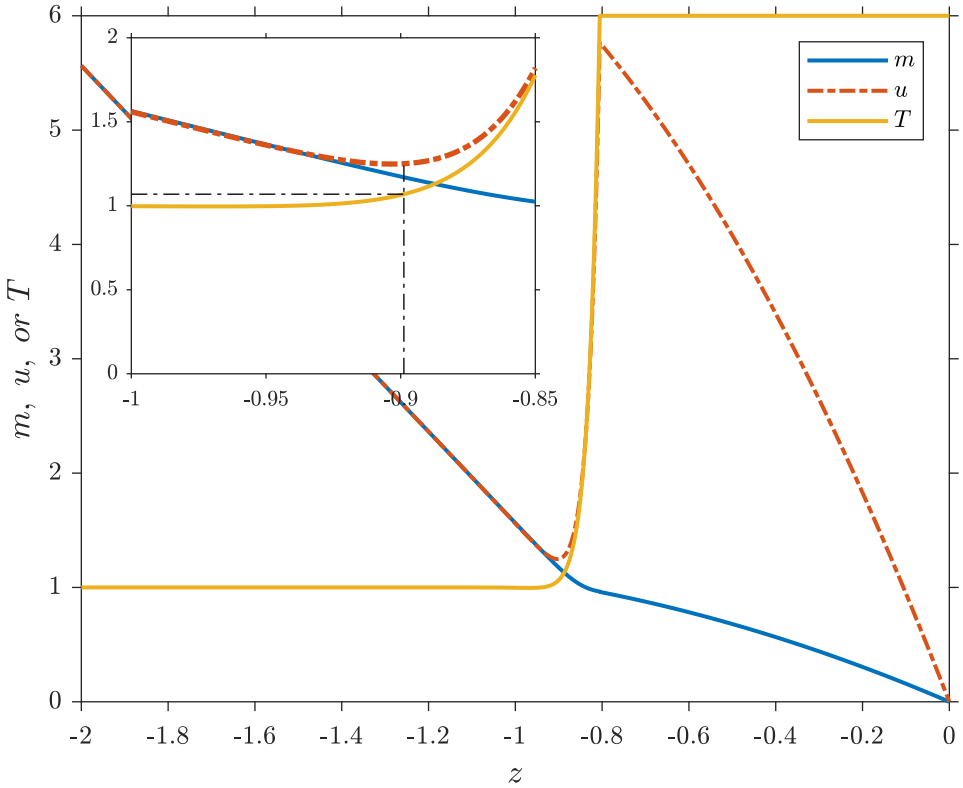

Figure 4.5: Variation of m, u and T across the flame for $\sigma = 6$ and $\delta = 0.025$

Experimentalists use three primary locations for measuring the gas velocity for determining the flame displacement speed (FDS). They are: (i) the location of minimum velocity ($\bar{z}$), (ii) the location of maximum velocity (z^{**}), and (iii) the location where the temperature has increased to some percentage of the unburned temperature (z^{*}). Since the maximum velocity occurs at a position/iso-surface sufficiently close to the reaction sheet ($T^{*} \approx \sigma$), the flame speed evaluated at z^{**} can be approximated by the flame speed at the reaction sheet ($z^{*} = -d$).

Figure 4.6 plots the flame speed evaluated at different locations or isotherms as a function of the flame stretch. The curves are linear as expected, and slopes of the curves are the Markstein lengths at those locations. As expected from equation (1.4), the non-dimensional laminar flame speed, $S_L = 1$, is recovered at zero flame stretch. Since $\mathcal{L}$ approaches large negative numbers for locations on the unburned side where $\theta \approx 1$, the flame speed evaluated at these locations increases with stretch rate. As the choice of isotherm shifts towards the reaction sheet, $\mathcal{L}$ approaches a constant value of $\mathcal{L}^b$ as seen from Figure 4.4. The rate of change of $\mathcal{M}$, and consequently $\mathcal{L}$, with position is rapid until a location close to the reaction sheet is achieved. Therefore, in order to

evaluate flame displacement speed of a stagnation point flame consistently, experimentalists should measure the gas velocity at a location that is very close to the reaction sheet or the burned side of the flame. Since the gas velocity is maximum at a location very close to the reaction sheet of the flame, the location of maximum velocity (z^{**}) can also be used to measure FDS consistently.

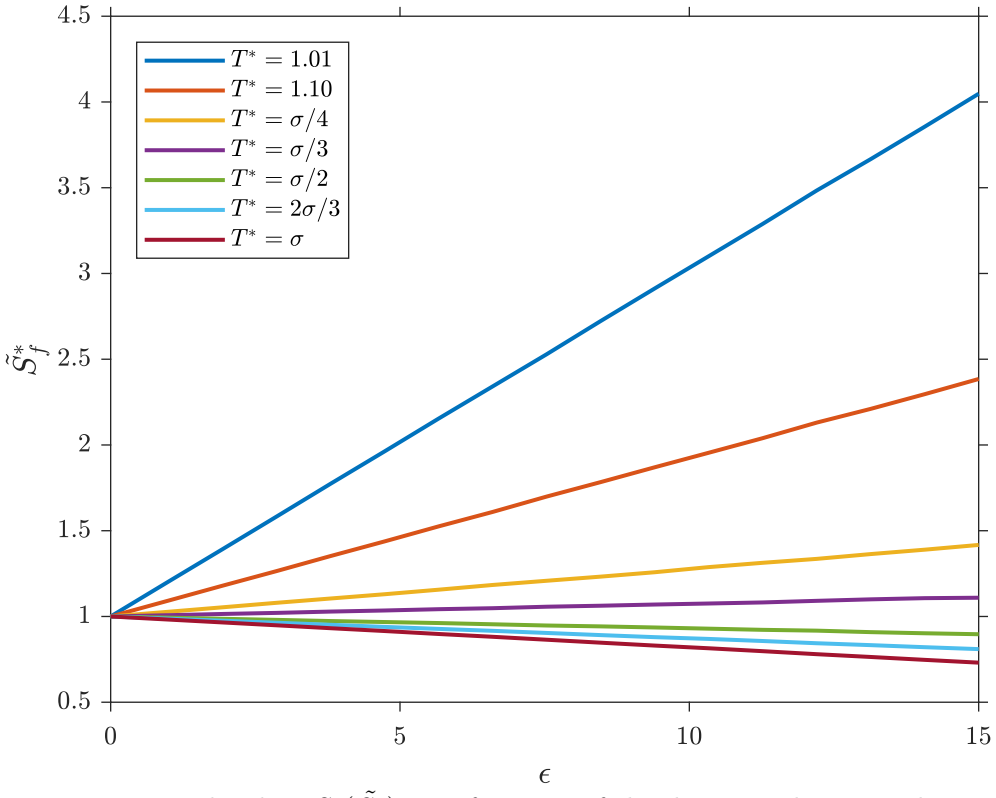

Figure 4.6: Normalized FDS ($\tilde{S}_f^*$) as a function of the dimensionless stretch rate ϵ

Using the location of minimum velocity, $\bar{z}$, as the upstream edge of the flame and measuring the flame speed at this location will give erroneous results. Figure 4.7 below shows the variation of normalized flame displacement speed measured at $\bar{z}$ with stretch rate. Similar to Figure 4.6, when the flame stretch is zero, the normalized flame displacement speed (FDS) is unity, as indicated by the blue curve in the figure below. Even though the temperature value at the minimum velocity location was found to be approximately 1.1 for $\sigma = 6$ and the $\tilde{S}_f^*$ versus ϵ plot for that case was linear, the curve in Figure 4.7 is non-linear for small values of ϵ; this is a violation of the linear trend predicted by equation (1.4). This non-linear trend can be explained by the fact that z^{**} varies non-linearly with flame stretch [5]. However, the non-linear trend seems to wear off as ϵ becomes sufficiently large, and the normalized FDS varies linearly with flame stretch for sufficiently large values of stretch rate. Figure 4.7 also plots the linear portion of the curve extrapolated to

zero stretch. Experimentalists sometimes utilize a similar technique to estimate the laminar flame speed. Nonetheless, as can be seen from the figure, the flame displacement speed evaluated by linear extrapolation of $\tilde{S}_f^*$ to zero stretch does not correspond to the laminar flame speed due to the initial non-linear behavior. Therefore, experimentalists should not choose the minimum gas velocity location for estimating the flame speeds.

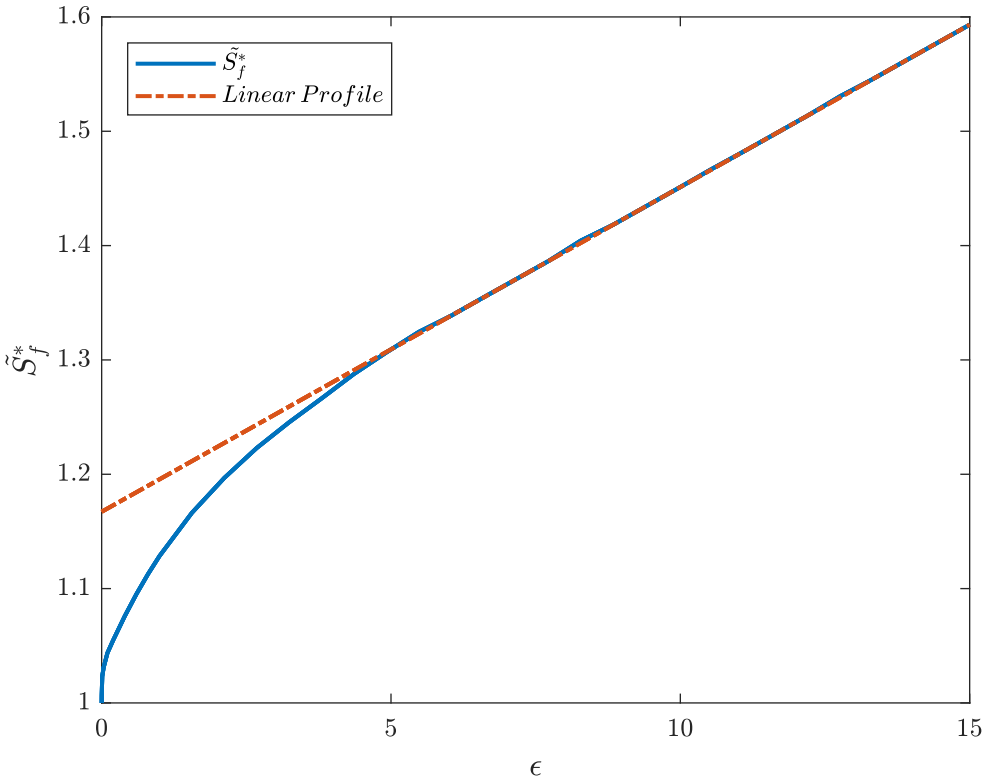

Figure 4.7: Normalized FDS ($\tilde{S}_f^*$) at position of minimum velocity as a function of ϵ

Chapter 5

CONCLUSION

The flow across a premixed flame in an axisymmetric laminar stagnation point flow was studied by resolving the structure of the pre-heat or flame zone and thereby accounting for diffusion of heat and mass. Initially, the problem was solved in a hydrodynamic sense where the diffusion effects were neglected and jump conditions derived from the conservation equations were used to relate the flow variables on the burned and unburned sides. Solutions for normal mass flux m, axial velocity u, radial velocity v, vorticity ω and pressure p were derived accurate to the order of the thickness of the flame. From this outer solution, it was found that vorticity (ω) is generated across the flame and that the quantity ω/r is a constant on the burned side of the flame. Additionally, expressions for the flame-standoff distance (d) and virtual stagnation point location (a) were derived, and the thermal expansion parameter, σ, was found to have a positive correlation with the flame-standoff distance.

Since the outer solutions for the flow variables were discontinuous at the location of the flame, inner solutions were presented for the variables m, T, ρ and u. The inner solutions were obtained by resolving the structure of the flame zone, which was in turn done by rescaling the outer coordinate by accounting for the diffusion length scale (δ). Additionally, in obtaining the inner solution, the reaction zone was assumed to be a thin sheet and therefore chemical kinetics were ignored. The inner and outer solutions were then matched and manipulated to obtain composite solutions or expressions for m and u. These composite solutions are valid everywhere in the flow domain except at the reaction sheet; hence, they have a discontinuity in slope at the position $z=-d$ which corresponds to the location of the reaction sheet.

The composite expression for axial velocity evaluated at the position $z^*=-d+\delta I(\eta)$ will give the flame displacement speed (S_f^*) at that location. However, in order to make a relevant comparison between the flame displacement speeds (FDS) evaluated at different locations, a density weighted FDS ($\tilde{S_f^*}$) was defined. The composite expression for the mass flux was used to derive an expression

for $\tilde{S}_f^*$, and from this, an expression for the Markstein length $\mathcal{L}^*$ was derived. It was shown that $\mathcal{L}^*$ approaches a constant value near the reaction sheet and becomes negative at locations where $T \approx T_u$. Subsequently, $\tilde{S}_f^*$ was plotted as a function of flame stretch and the relation was proved to be linear at several locations within the flame zone determined by isotherms. However, the FDS evaluated at locations close to the unburned side of the flame had positive slopes which violated the theoretical prediction. This contradiction was explained using the variation of $\mathcal{L}$ across the flame zone and the fact that $\mathcal{L} < \mathcal{L}^b$ for $z < -d$. In addition, the normalized flame displacement speed evaluated at the location of minimum velocity was found to have a non-linear relationship with flame stretch. Due to these inconsistencies with measurement of FDS on the unburned side, a recommendation was provided to measure the FDS at locations sufficiently close to the reaction sheet in experiments.

The present study has provided results that are accurate everywhere except the reaction zone, but it did not consider the chemical kinetics of the fuel-oxidizer mixture. In order to have a better understanding of the chemical kinetics, a numerical simulation of the problem using a detailed model for the chemical kinetics needs to be performed using a package such as *Cantera*.

REFERENCES

[1] George K. Giannakopoulos, Athanasios Gatzoulis, Christos E. Frouzakis, Moshe Matalon, and Ananias G. Tomboulides. Consistent definitions of "Flame Displacement Speed" and "Markstein Length" for premixed flame propagation. *Combustion and Flame*, 162(4):1249–1264, 2015.

[2] Moshe Matalon. Flame dynamics. *Proceedings of the Combustion Institute*, 32 I(1):57–82, 2009.

[3] Moshe Matalon. On Flame Stretch. *Combustion Science and Technology*, 31(3-4):169–181, 1983.

[4] C. K. Wu and C. K. Law. On the determination of laminar flame speeds from stretched flames. *Symposium (International) on Combustion*, 20(1):1941–1949, 1985.

[5] J. H. Tien and M. Matalon. On the burning velocity of stretched flames. *Combustion and Flame*, 84(3-4):238–248, 1991.

[6] M. Matalon and B. J. Matkowsky. Flames as gasdynamic discontinuities. *J. Fluid Mech.*, 124(1982):239–259, 1982.

[7] J. K. Bechtold and M. Matalon. The dependence of the Markstein length on stoichiometry. *Combustion and Flame*, 127(1-2):1906–1913, 2001.

[8] L. Howarth. CXLIV. The boundary layer in three dimensional flow. Part II . The flow near a stagnation point. *The London, Edinburgh, and Dublin Philosophical Magazine and Journal of Science*, 42(335):1433–1440, 1951.

[9] M. Matalon, C. Cui, and J. K. Bechtold. Hydrodynamic theory of premixed flames: effects of stoichiometry, variable transport coefficients and arbitrary reaction orders. *Journal of Fluid Mechanics*, 487:179–210, 2003.

[10] E. Eteng, G. S. S. Ludford, and M. Matalon. Displacement effect of a flame in a stagnation-point flow. *Physics of Fluids*, 29(7):2172–2180, 1986.

[11] Moshe Matalon and John K. Bechtold. A multi-scale approach to the propagation of non-adiabatic premixed flames. *Journal of Engineering Mathematics*, 63(2-4):309–326, 2009.